NATIONAL ADVISORY COMMITTEE FOR AERONAUTICS

REPORT 1227

AN INVESTIGATION OF THE MAXIMUM LIFT OF WINGS AT SUPERSONIC SPEEDS

By JAMES J. GALLAGHER and JAMES N. MUELLER

1955

For sale by the Superintendent of Documents, U.S. Government Printing Office, Washington 25, D.C. Yearly subscription, $10; foreign, $13; single copy price varies according to size - - - - - - - - - Price 30 cents

REPORT 1227

AN INVESTIGATION OF THE MAXIMUM LIFT OF WINGS AT SUPERSONIC SPEEDS

By JAMES J. GALLAGHER and JAMES N. MUELLER

Langley Aeronautical Laboratory
Langley Field, Va.

National Advisory Committee for Aeronautics

Headquarters, 1512 H Street NW., Washington 25, D. C.

Created by act of Congress approved March 3, 1915, for the supervision and direction of the scientific study of the problems of flight (U. S. Code, title 50, sec. 151). Its membership was increased from 12 to 15 by act approved March 2, 1929, and to 17 by act approved May 25, 1948. The members are appointed by the President, and serve as such without compensation.

REPORT 1227

AN INVESTIGATION OF THE MAXIMUM LIFT OF WINGS AT SUPERSONIC SPEEDS[1]

By James J. Gallagher and James N. Mueller

SUMMARY

An exploratory investigation was carried out in the Langley 9-inch supersonic tunnel to determine the maximum lift of wings operating at supersonic speeds. A variety of wing plan forms of random thickness distributions were tested at Mach numbers of 1.55, 1.90, and 2.32 and at Reynolds numbers varying between 0.74×10^6 and 0.27×10^6 at angles of attack ranging from zero up through the angle at which maximum lift occurred. In general, at these Mach numbers the value of maximum lift coefficient was approximately 1.05+ 0.05; it appeared to be independent of plan form and decreased slightly with increasing Mach number. No discontinuities in lift occurred from zero angle of attack through maximum lift, which was attained at an angle of attack of approximately 40°. In the Mach number range tested, the lift curves remained linear for angles of attack as high as 20° to 30°. Lift-drag ratios at maximum lift were of the order of 1.0.

Subsequent pressure-distribution tests on wings of triangular and rectangular plan forms were made at a Mach number of 2.40. The results of these tests substantiated the values of maximum lift obtained during the force tests and further showed no appreciable center-of-pressure shift over the entire angle-of-attack range.

INTRODUCTION

The designer of supersonic aircraft—particularly the guided-missile designer—is interested in the maximum loads that can be withstood on wings operating at supersonic speeds. The need for such maximum-load information is obvious in determining the maximum accelerations that can be withstood by supersonic aircraft and in the structural design of aircraft components. In order to provide maximum-lift and drag information, force tests of 11 wings were made in the Langley 9-inch supersonic tunnel up to high angles of attack. Only available models were used; hence, no comprehensive study of plan form or wing section was made. Subsequent tests were made on two pressure-distribution models of rectangular and triangular plan forms.

SYMBOLS

A	aspect ratio, b^2/S
b	maximum wing span, ft
C_D	drag coefficient, Drag/qS
C_L	lift coefficient, Lift/qS
C_m	pitching-moment coefficient, Pitching moment/qSc
c	maximum wing chord measured in streamwise direction, ft
M	stream Mach number
P	pressure coefficient, $\frac{p_l-p}{q}$
p	stream static pressure, lb/sq ft
p_l	local static pressure, lb/sq ft
q	stream dynamic pressure, $\frac{1}{2}\rho V^2$, lb/sq ft
R	Reynolds number referred to c, $\rho Vc/\mu$
S	wing area, sq ft
t	maximum thickness of wing, ft
t/c	thickness ratio of wing in stream direction
V	stream velocity, ft/sec
y	spanwise coordinate measured from wing center line, ft
α	angle of attack, deg
ϵ	triangular-wing semivertex angle, deg
θ	wing-tip angle measured from stream direction, deg
Λ	sweep angle of leading edge, deg
μ	stream viscosity, lb-sec/ft^2
ρ	stream density, slugs/cu ft

APPARATUS AND TEST METHODS

DESCRIPTION OF TUNNEL

The Langley 9-inch supersonic tunnel is a closed-return wind tunnel in which the humidity and temperature of the air can be controlled with suitable drying and cooling equipment. The test Mach number is varied by the use of interchangeable nozzle blocks which form test sections approximately 9 inches square. Models are mounted in the tunnel on shielded stings, and the forces are measured on a three-component balance system. The range of the externally controllable angle-of-attack mechanism is ±5°.

DESCRIPTION OF MODELS AND SUPPORTS

The force-test models are shown in figure 1, and pertinent dimensions are given in table I. The two trapezoidal wings ($\theta=30°$ and $\theta=40°$) were made by obliquely cutting off the tips of rectangular wings which had symmetrical circular-arc airfoil sections. The trapezoidal wings were tested with both blunt and beveled tips. The rectangular wings had symmetrical circular-arc airfoil sections. The 63° and 45° swept wings had modified symmetrical circular-arc airfoil sections perpendicular to the leading edges. The modifica-

[1] Supersedes recently declassified NACA RM L7J10, 1947.

tions entailed rounding the leading edges and beveling the tips. The 36° swept wing had the same airfoil section and tip bevel as the other swept wings, but its tips were cut off parallel to the stream direction. The triangular wings were flat plates with the leading edges beveled slightly and rounded off and the trailing edges beveled to a sharp edge. A more complete description of the 63° and 45° swept and triangular wings is given in reference 1.

Various stings (fig. 2) were used to support the models for the force tests. Most of the tests were made with stings shielded by the short windshield shown in figure 3; however, some tests were made with the long windshield shown in figure 4. The combinations of the various wings and their supports are summarized in table II.

Photographs of the pressure-distribution models are shown as figure 5, and pertinent dimensions are given in table I. Measurements of the pressure distribution over the wing were made by means of orifices located in one surface of the semispan of the wings at the positions shown in figure 6. A complete set of orifices was placed in only one surface in order to simplify the design and construction of the models.

These pressure-distribution models were supported from the side walls of the tunnel by means of struts. The struts were hinged from the side wall of the tunnel to provide a means for changing the angle of attack and served as conduits for the pressure tubes.

TEST METHODS

Because of the limited range of the tunnel angle-of-attack mechanism ($\pm 5°$), some means which would allow higher angles to be reached had to be devised for the force tests. The angle-of-attack range was covered by bending the stings (fig. 2) successively in 10° increments and filling in smaller incremental angles with the angle-of-attack mechanism.

The first set of data taken at $M=2.32$ by using sting A showed displacements of successive groups of test points in the lift results as shown in figure 7. These displacements in the lift results suggested that the forces on the sting might be larger than had originally been expected. The maximum displacement of the test-point groups in the region of maximum lift occurred for the wing of smallest area (fig. 7 (b)) and was of the order of 6 percent. In general, only small displacements are to be noted in the drag curves.

Because of the displacements in the test-point groups indicated in the results at $M=2.32$ when sting A was used, sting B (fig. 2) was used in the next series of tests at $M=1.55$ (fig. 8) in an attempt to reduce the forces on the model support. The maximum displacement of the test-point groups in the region of maximum lift occurred, as in the tests at $M=2.32$, for a wing of small area but was about 5 percent (fig. 8 (b)). The displacements for most of the configurations, however, were considerably less. The displacements in the drag test-point groups were again small as compared with those in the lift results.

Although the shorter sting reduced the magnitude of the discontinuities in the lift curves, the absolute values of the forces on the model supports were still not known. In an attempt to evaluate these forces, eight pairs of static orifices were installed on sting B and tests were made at $M=1.55$ for the configurations indicated in table II. The corrected lift data are shown in figures 8 (a), 8 (b), 8 (f), and 8 (g). The long windshield was also used in tests in an attempt to minimize the forces on the model support as much as possible and to provide an additional comparative value of lift close to maximum lift.

The tests at $M=1.55$ showed good agreement between the values of maximum lift obtained by correcting for the sting pressures and by using the long windshield; therefore, in the next series of tests, the long windshield was used to obtain check data. For the tests at $M=1.90$, sting B was again employed and, because of the reduction in the magnitude of the lift-curve displacements in going from sting A to sting B, a still shorter model support, sting C, was also employed. The tests at $M=1.90$ were made at angles of attack in the region of maximum lift only. (See fig. 9.)

During the pressure-distribution tests, data were obtained on the models by varying the angle of attack of the configurations through the desired range. Because the wing was equipped with pressure orifices on only one surface of the semispan, it was necessary, in order that complete pressure distributions might be obtained, to make tests at both positive and negative angles of attack. Subsequently, the data at negative and positive angles of attack were combined to form complete pressure diagrams such as those shown in figure 10.

PRECISION OF DATA

It should be realized that the primary purpose of the tests was to obtain values of maximum lift. Data obtained at the lower angles were not expected to be so accurate as those obtained at the higher angles because the test technique employed was one of convenience. Furthermore, no reasonable values of pitching moment for the force tests were obtained because the lack of sufficient instrumentation made it impossible to evaluate the magnitude and location of the resultant force on the sting.

The total forces on the models and supports were measured on self-balancing beam scales. The maximum probable errors in the scale measurements are of the order of a small fraction of 1 percent of the forces at maximum lift and thus appear to be negligible in comparison with the other errors involved in evaluating the forces on the model supports. The differences in values obtained by the various model-support schemes thus remain the only means of judging the accuracy of the maximum-lift results.

From the considerations of the various factors entering into the pressure measurements made on the wings, the final values of pressure coefficient P are estimated to represent conditions existing in the tests to within ± 0.005. Because of uncertainties involved in fairing and integrating the pressure-distribution diagrams, the integrated force coefficients are less accurate than the pressure measurements themselves, although quantitative limits are difficult to define.

MAXIMUM LIFT

The lack of any previous information on maximum lift at supersonic Mach numbers made the check tests in this

investigation necessary. Most of the information regarding accuracy was obtained at $M=1.55$; however, some additional checks were made at $M=1.90$. At maximum lift the data, corrected on the basis of a few pressure measurements on the sting (shown in figs. 8 (a), 8 (b), 8 (f), and 8 (g)), checked the uncorrected lift values to within 5 percent, except for the trapezoidal wing for which there was an 8-percent discrepancy. The pressure forces could have been evaluated precisely by taking sufficient pressure readings along the sting but the process would have been prohibitively tedious. Thus, because of the unknown precision of evaluating the lift component of the sting pressure forces, an evaluation of the precision of the uncorrected results is not directly possible. The fact that the pressure corrections have taken most of the 10°-increment displacements out of all the lift curves (with the exception of fig. 8 (b)) does, however, lend credence to the validity of the pressure corrections.

It appears from the data that the difference between the uncorrected and corrected values of maximum lift is indicated as a reduction in the corrected value of about 5 percent. The data obtained with the long windshield covering the stings fell between the uncorrected data and the data corrected by use of the sting pressures. The long-windshield data differed by 2 to 4 percent from the uncorrected data with the exception of the trapezoidal wing which still disagreed by about 8 percent. Further check tests at $M=1.90$ (fig. 9) with the long windshield checked the uncorrected lift data obtained with sting B within approximately 7 percent or less, and sting C, within 3 to 4 percent. Since, in general, the various methods show a scatter in the order of 0.05 for maximum lift coefficient, it is felt that the results are probably significant to 0.05.

DRAG AT MAXIMUM LIFT

An insufficient number of pressure tubes were installed on the stings to allow a reasonable value of sting drag to be obtained from integration of these pressures. The only method thus available of evaluating the accuracy of the sting drag is by comparing data obtained with the long and the short spindle windshields. Figures 8 (a), 8 (b), 8 (f), and 8 (g) show that the uncorrected drag obtained with the short spindle windshield is about 4 to 8 percent higher than the data obtained with the long windshield. Tests made at $M=1.90$ show approximately the same error (fig. 9).

LIFT AT LOW ANGLES

The magnitude of the sting forces at the lower angles of attack could not be very easily evaluated; thus, data in reference 1 for identical wings with short stings are used for a check. The only wings in reference 1 for which a reasonable angle-of-attack range was tested were the triangular wings ($\epsilon=26°$ and $\epsilon=45°$) at $M=1.43$ and $M=1.71$. Comparisons of low-angle data ($\alpha=0°$ to 4°) show that the values of the lift and lift-curve slopes herein presented at $M=1.55$ with sting B are about 9 to 11 percent lower than those in reference 1, for which a direct interpolation for Mach number was made. Although the two configurations do not afford conclusive evidence as to the accuracy of the data, the other data will probably compare equally as well in precision. Furthermore, the checks were made with the wings of smaller area for which the sting forces represent a greater percentage of the total force; thus, the data for the wings of larger area are probably more accurate.

DRAG AT LOW ANGLES

Drag checks at the lower angles of attack similar to the lift checks were made by using the data presented in reference 1. The values of drag coefficient ($M=1.55$) with sting B were compared with those of reference 1. The drag-coefficient values obtained from reference 1 were corrected as indicated therein.

Values of minimum drag coefficient presented in this report are approximately 0.01 higher than those of reference 1. This higher drag is probably due to differences between the sting configurations. The stings in the present tests were much longer than those in reference 1; in addition, at zero lift, the sting for the wings in reference 1 was at an angle of attack of 0°, whereas, for the present data at zero lift, the rear portions of the stings were at an angle of attack of −5°. Values of minimum drag coefficient taken from the curves in this report will probably be too high and of doubtful value.

STREAM SURVEYS

Stream surveys have indicated slight variations in stream Mach number and static pressure in the test section. The maximum variations measured for the test sections of the nozzles used in these tests are as follows:

Mach number	Maximum variation in Mach number, percent	Maximum variation in stream pressure, percent
1.55	±0.6	±1.3
1.90	±0.5	±1.5
2.32	±0.4	±1.5
2.40	±0.5	±1.5

It is felt that these variations do not affect the data to a sufficient extent to warrant discussion relative to the present tests.

RESULTS AND DISCUSSION

Force and pressure-distribution results for the various wings tested are presented in figures 8, 9, 7, and 11 for Mach numbers of 1.55, 1.90, 2.32, and 2.40, respectively. The Reynolds number per inch of chord for the test models varied between 0.37×10^6 at $M=1.55$ and 0.26×10^6 at $M=2.40$. The maximum Reynolds number attained in these tests was 0.74×10^6 for the 63° sweptback wing at a Mach number of 1.55.

LIFT RESULTS

Maximum-lift region.—The value of the maximum lift coefficient for all force-test configurations was practically constant for each Mach number regardless of the plan form. The maximum lift coefficient did vary slightly with Mach number and tended to decrease as the Mach number became greater. At a Mach number of 1.55, an average value of maximum lift coefficient for all configurations of approximately 1.10 was obtained; this value decreased to 1.05 at $M=1.90$ and decreased further to 1.00 at $M=2.32$. Table III summarizes the values of maximum lift coefficient for the various configurations at each Mach number. The

angle of attack at which maximum lift coefficient occurred was approximately 40° for all Mach numbers and configurations, and the lift curves remained continuous throughout the angle-of-attack range.

In figure 11 the lift results obtained for wings of rectangular and triangular plan forms by means of pressure-distribution measurements are shown. The maximum lift coefficients obtained for the pressure-distribution wings corroborates the force data.

Low-angle region.—The experimental lift curves, when faired through the intermediate values of each test-point group, are linear up to angles of attack as high as 20° for the 63° sweptback wing at $M=1.55$ and to 30° for the triangular ($\epsilon=26°$) and 63° sweptback wings at $M=2.32$. In general, the trend of the lift curves for all the wings was to remain linear to higher angles of attack as the Mach number increased. Comparisons of theoretical and experimental lift-curve slopes show the theoretical slopes to have deviations from a maximum of 50 percent greater (for the trapezoidal wing, $\theta=40°$, and tips beveled) to 6 percent less (for the trapezoidal wing, $\theta=30°$, and tips not beveled) than the experimental slopes.

The experimental lift-curve slopes herein presented for the triangular wings ($\epsilon=26°$ and $\epsilon=45°$) at $M=1.55$ show deviations of 10 to 20 percent, respectively, less than the linear theory, as compared with corresponding deviations of approximately 18 percent greater and 10 percent less for identical triangular wings of reference 1 at $M=1.43$.

No general consistency is observed between the experimental and theoretical lift curves among the various plan forms or for given plan forms at the different Mach numbers.

DRAG RESULTS

The drag tare forces appear to be much more influenced by sting length than the lift forces in the maximum-lift region, and an insufficient number of check points were obtained to give any reasonable value of drag coefficient for which a comparison could be made.

The value of the drag coefficient obtained at maximum lift is approximately 1.0; however, no significant indication of the variation of drag for any configuration with Mach number can be deduced because of the different sting lengths used at the various test Mach numbers.

Lift-drag ratios of the order of 1.0 were obtained at maximum lift. No significant differences in the value of this ratio are noted with change in plan form and Mach number.

CENTER-OF-PRESSURE RESULTS

The variation of the center of pressure over the angle-of-attack range is shown in figures 11 (a) and 11 (b) for the rectangular and triangular wings, respectively, used for the pressure-distribution tests. The results indicate an almost negligible change in location of the center of pressure over the entire angle-of-attack range for the rectangular wing and show an overall rearward travel of about 6 percent c for the triangular wing.

SCHLIEREN PHOTOGRAPHS

Schlieren photographs of plan and side views of two of the configurations at $M=1.55$ are shown in figure 12 with both vertical and horizontal knife edges. The pictures mainly show by the strong shock ahead of the wing that, as would be expected, the wings constitute a very large disturbance to the flow. It appears that not a great deal can be learned from these schlieren photographs because the flow about the wing is three-dimensional.

CONCLUSIONS

Supersonic-tunnel force tests to determine the maximum lift of 11 wings of various plan forms and thickness distributions at Mach numbers of 1.55, 1.90, and 2.32 and at Reynolds numbers varying between 0.74×10^6 and 0.27×10^6 have indicated the following conclusions:

1. The average value of maximum lift coefficient was approximately 1.05 ± 0.05 and appeared to have no significant variation with plan form; however, the value decreased slightly with increasing Mach number.
2. The lift curve remained linear for angles of attack as high as 20° to 30°, and no discontinuities in lift occurred from zero up to and slightly above maximum lift.
3. Maximum lift was not obtained until an angle of attack of approximately 40° was reached.
4. Lift-drag ratios of approximately 1.0 were obtained at maximum lift.

Pressure-distribution tests conducted at a Mach number of 2.40 and Reynolds number of about 0.6×10^6 to determine the maximum lift of a rectangular and a triangular wing have indicated the following conclusions:

1. The pressure-distribution results corroborate closely the maximum lift values obtained in the force tests.
2. Center-of-pressure travel over the entire angle-of-attack range up to and including maximum lift was small.

LANGLEY AERONAUTICAL LABORATORY,
NATIONAL ADVISORY COMMITTEE FOR AERONAUTICS,
LANGLEY FIELD, VA., *October 17, 1947.*

REFERENCE

1. Ellis, Macon C., Jr., and Hasel, Lowell E.: Preliminary Investigation at Supersonic Speeds of Triangular and Sweptback Wings. NACA TN 1955, 1949.

TABLE I.—MODEL SHAPE PARAMETERS

Wing	Aspect ratio, A	Wing area, sq in.	Maximum chord in stream direction, in.	Thickness ratio, t/c
Triangular, $\epsilon=26°$	1.96	1.772	1.890	0.02
Triangular, $\epsilon=45°$	4.06	1.295	1.130	.03
Swept, $\Lambda=36°$	1.76	3.600	1.135	.11
Swept, $\Lambda=45°$	3.23	3.340	1.330	.09
Swept, $\Lambda=63°$	1.37	3.340	2.070	.06
Trapezoidal, $\theta=40°$	3.36	1.095	1.069	.06
Trapezoidal, $\theta=30°$	2.78	1.440	1.008	.09
Rectangular	1.74	1.972	1.069	.06
Rectangular	1.99	2.019	1.008	.09
Rectangular [a]	2.29	6.980	1.745	.09
Triangular [a]	2.45	5.552	3.011	.10

[a] Pressure-distribution model.

TABLE II.—TEST CONFIGURATIONS

Wing	Sting	Spindle windshield	Mach number, M	Angle of attack, α, deg
Triangular, $\epsilon=26°$	B[a]	Short	1.55	0 to 52
	A	Long	1.55	45
	B	Short	1.90	40 to 52
	C	Short	1.90	40 to 52
	A	Long	1.90	45
	A	Short	2.32	0 to 50
Triangular, $\epsilon=45°$	B[a]	Short	1.55	0 to 50
	A	Long	1.55	48
	A	Short	2.32	0 to 52
Swept, $\Lambda=36°$	B	Short	1.55	0 to 44
	B	Short	1.90	46 to 56
	C	Short	1.90	42 to 56
	A	Long	1.90	46
Swept, $\Lambda=45°$	B	Short	1.55	0 to 45
	A	Short	2.32	0 to 50
Swept, $\Lambda=63°$	B	Short	1.55	0 to 41
	A	Short	2.32	0 to 52
Trapezoidal, $\theta=40°$, tips beveled	B[a]	Short	1.55	0 to 50
	A	Long	1.55	45
	B	Short	1.90	42 to 54
	C	Short	1.90	42 to 52
	A	Long	1.90	47
Trapezoidal, $\theta=40°$, tips not beveled	B	Short	1.55	0 to 12
Trapezoidal, $\theta=30°$, tips beveled	B	Short	1.90	40 to 50
	C	Short	1.90	40 to 50
Trapezoidal, $\theta=30°$, tips not beveled	C	Short	1.90	40 to 48
	A	Short	2.32	0 to 51
Rectangular, $A=1.74$	B[a]	Short	1.55	0 to 50
	A	Long	1.55	46
	B	Short	1.90	42 to 54
	C	Short	1.90	42 to 52
	A	Long	1.90	46
Rectangular, $A=1.99$	A	Short	2.32	0 to 52
Rectangular,[b] $A=2.29$	----	--------	2.40	0 to 42
Triangular,[b] $A=2.45$	----	--------	2.40	0 to 49

[a] Sting lift evaluated by sting pressures in region of maximum lift.
[b] Pressure-distribution model.

TABLE III.—MAXIMUM LIFT-COEFFICIENT VALUES

Wing	Maximum C_L		
	$M=1.55$	$M=1.90$	$M=2.32$
Triangular, $\epsilon=26°$	1.05	1.05	1.00
Triangular, $\epsilon=45°$	1.10	------	1.05
Swept, $\Lambda=36°$	1.10	1.00	----------
Swept, $\Lambda=45°$	1.10	------	.95
Swept, $\Lambda=63°$	1.00	------	.95
Trapezoidal, $\theta=40°$, tips beveled	1.15	1.10	----------
Trapezoidal, $\theta=30°$, tips not beveled	------	1.05	1.00
Trapezoidal, $\theta=30°$, tips beveled	------	1.05	----------
Rectangular, $A=1.74$	1.15	1.05	----------
Rectangular, $A=1.99$	------	------	1.00
Rectangular,[a] $A=2.29$	------	------	.95 ($M=2.40$)
Triangular,[a] $A=2.45$	------	------	.95 ($M=2.40$)

[a] Pressure-distribution model.

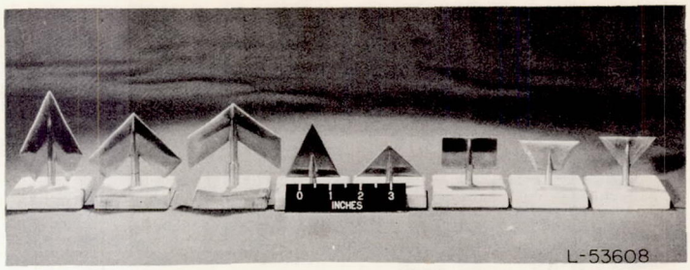

FIGURE 1.—General view of force-test models.

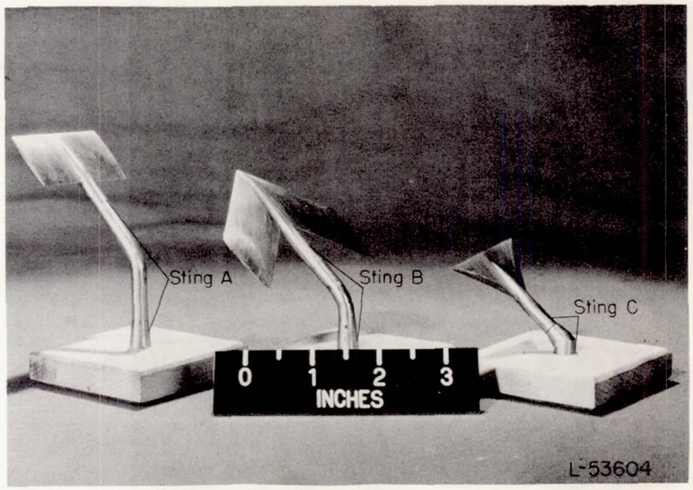

FIGURE 2.—Various stings used in tests. Stings bent 45°.

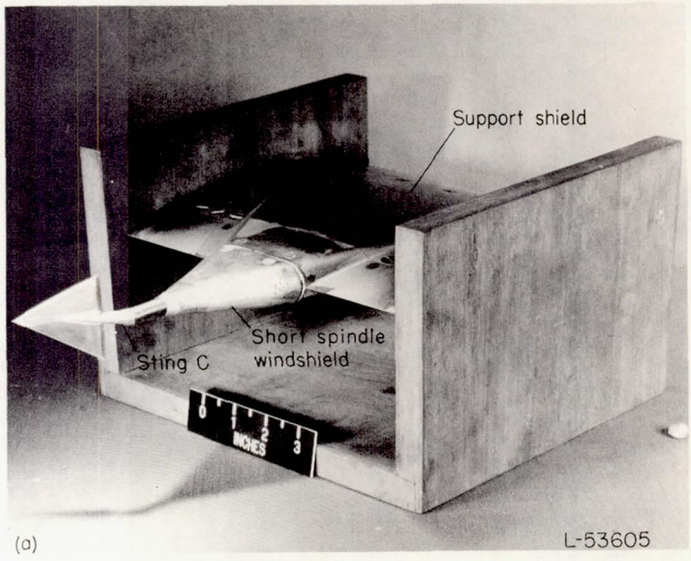

(a) Sting C.

FIGURE 3.—Triangular wing mounted on various stings, showing support shield and short spindle windshield used in the tunnel tests.

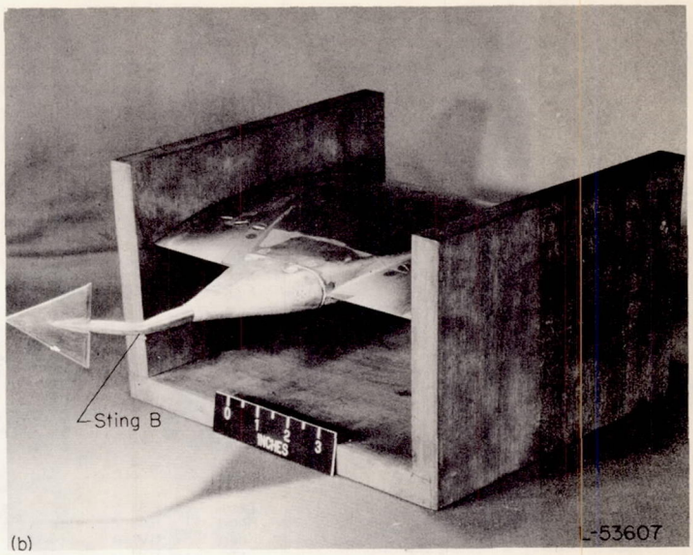

(b) Sting B.

FIGURE 3.—Concluded.

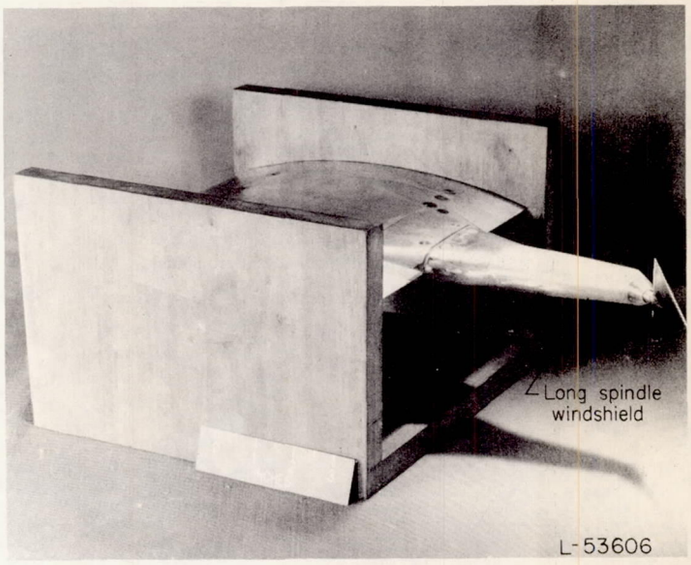

FIGURE 4.—Long spindle windshield used to cover sting supports.

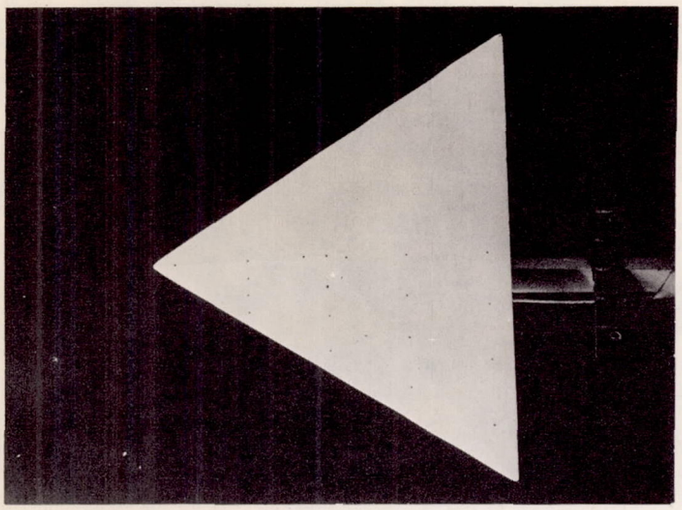

Top view L-85297

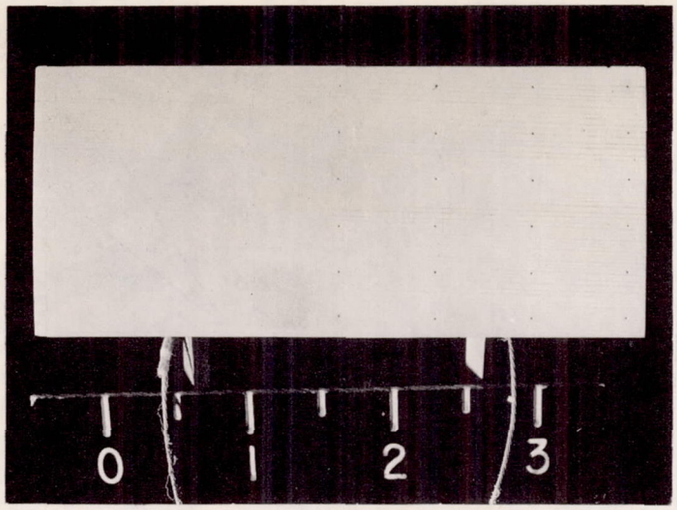

Top view L-8529

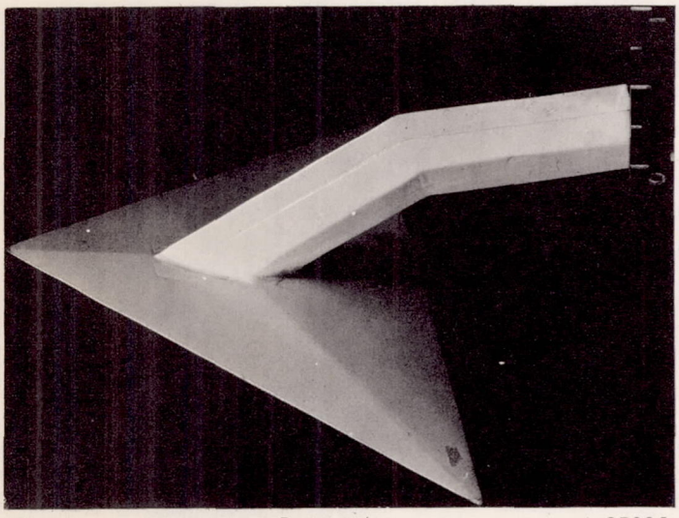

(a) Bottom view L-85298

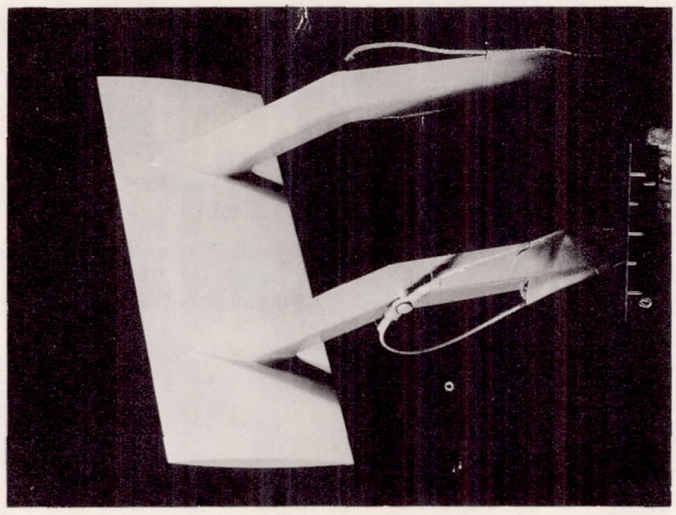

(b) Bottom view L-85295

(a) Triangular wing. (b) Rectangular wing.

FIGURE 5.—Photographs of pressure-distribution models.

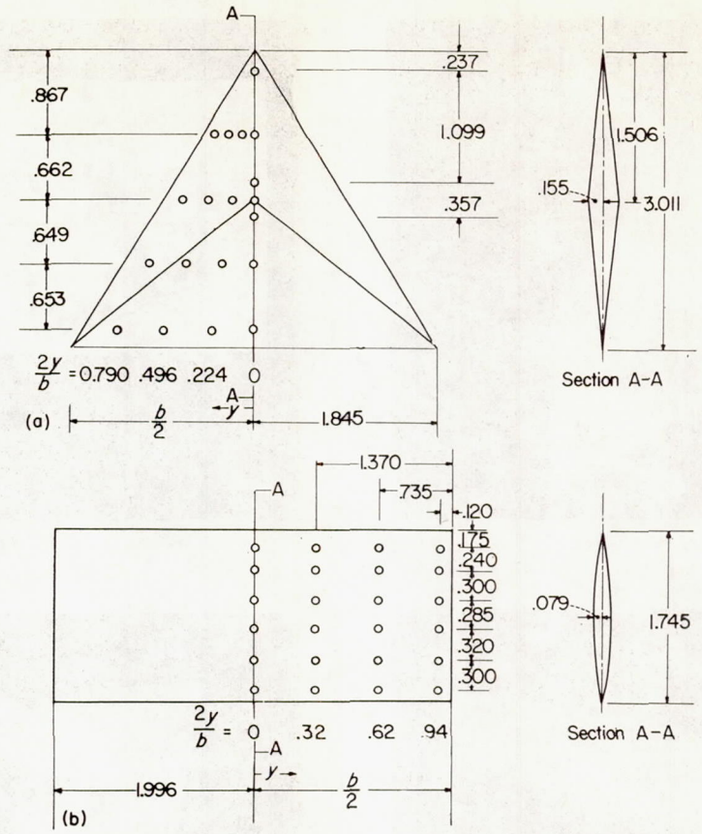

(a) Triangular wing; $\epsilon = 31.5°$. Double-wedge airfoil section.
(b) Rectangular wing. Circular-arc airfoil section.

FIGURE 6.—Dimensional sketches of pressure-distribution models.
(All dimensions are in inches.)

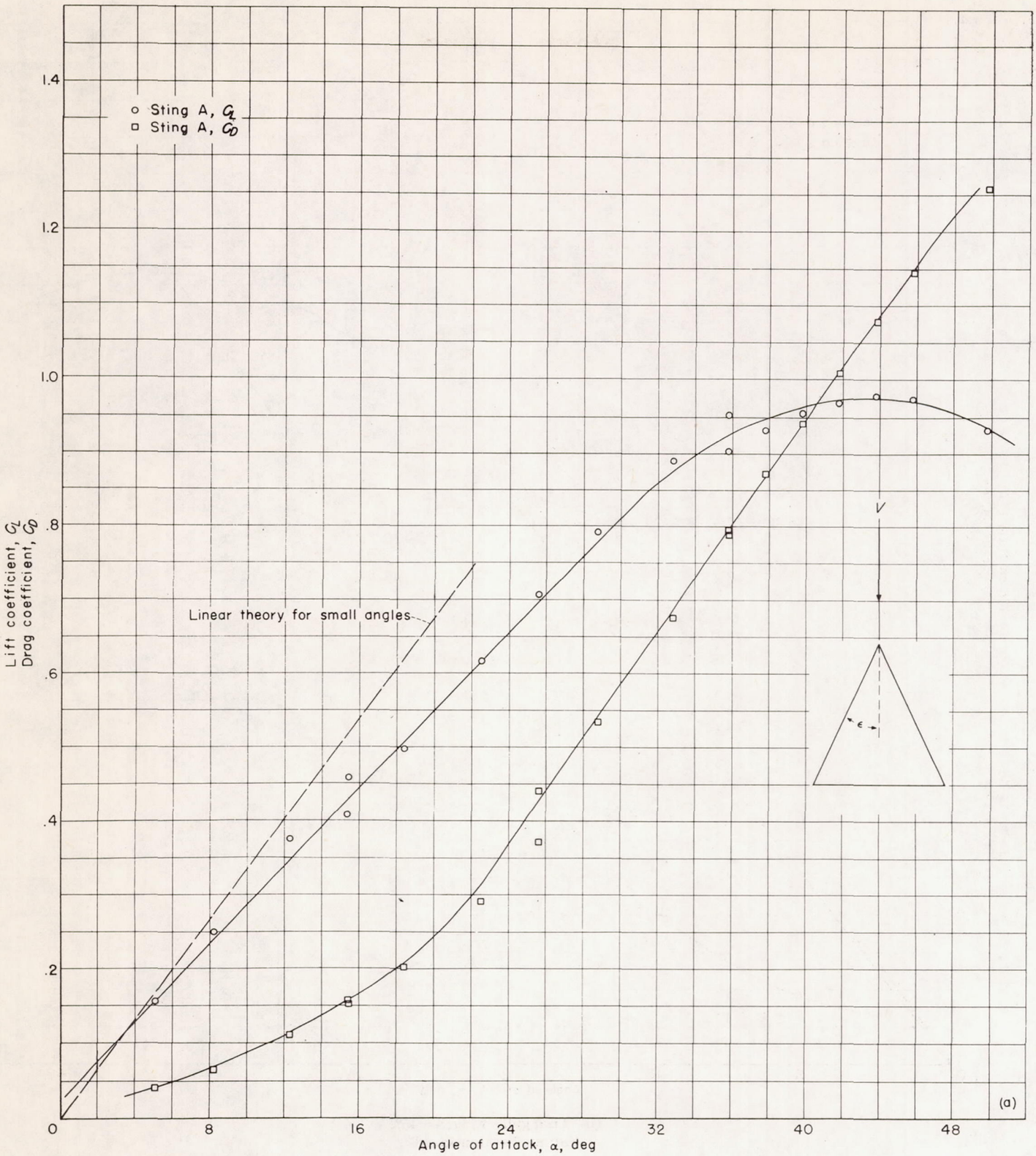

(a) Triangular wing; $\epsilon = 26°$.

FIGURE 7.—Variation of lift coefficient and drag coefficient with angle of attack. $M = 2.32$.

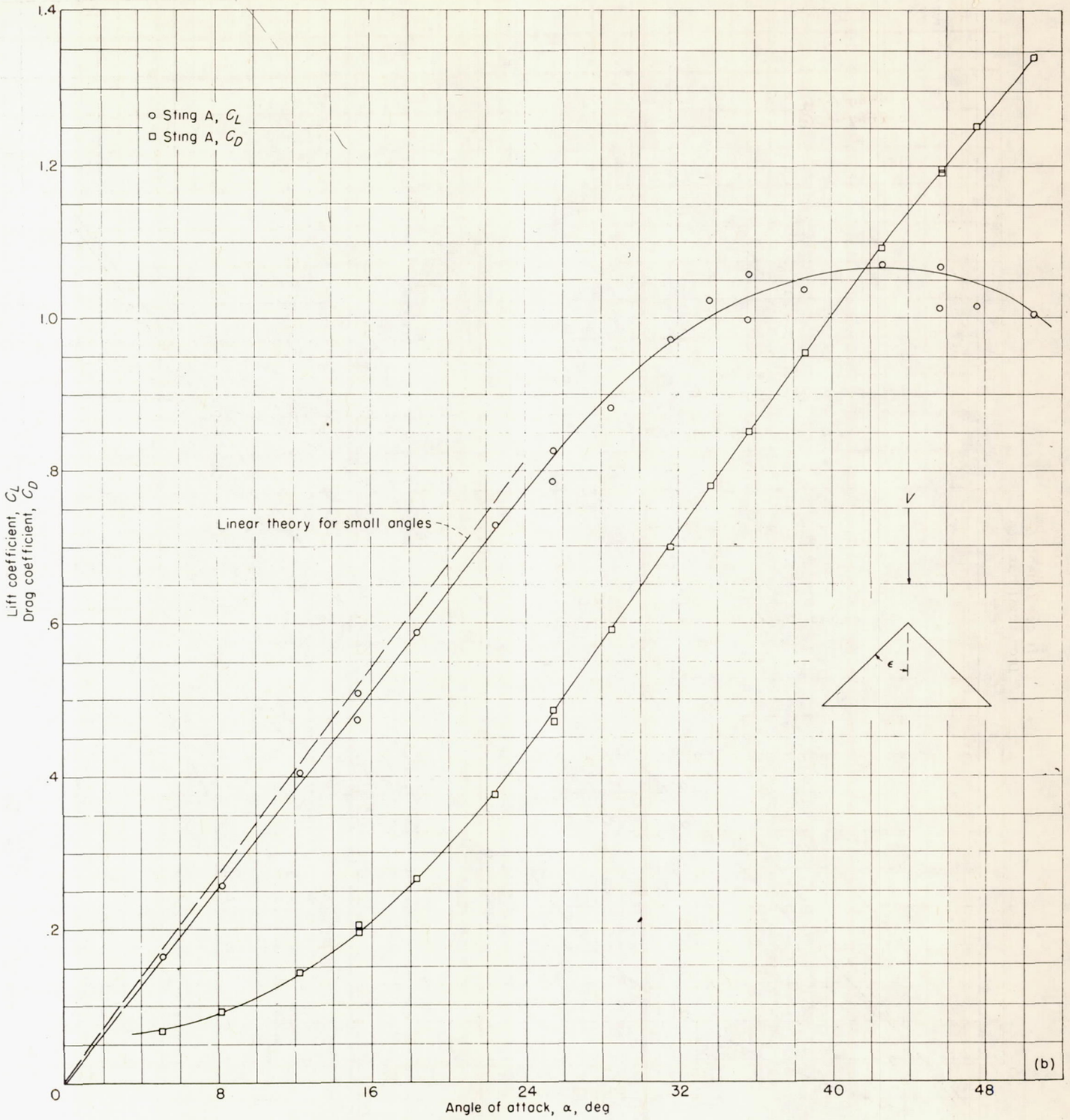

(b) Triangular wing; $\epsilon = 45°$.

FIGURE 7.—Continued.

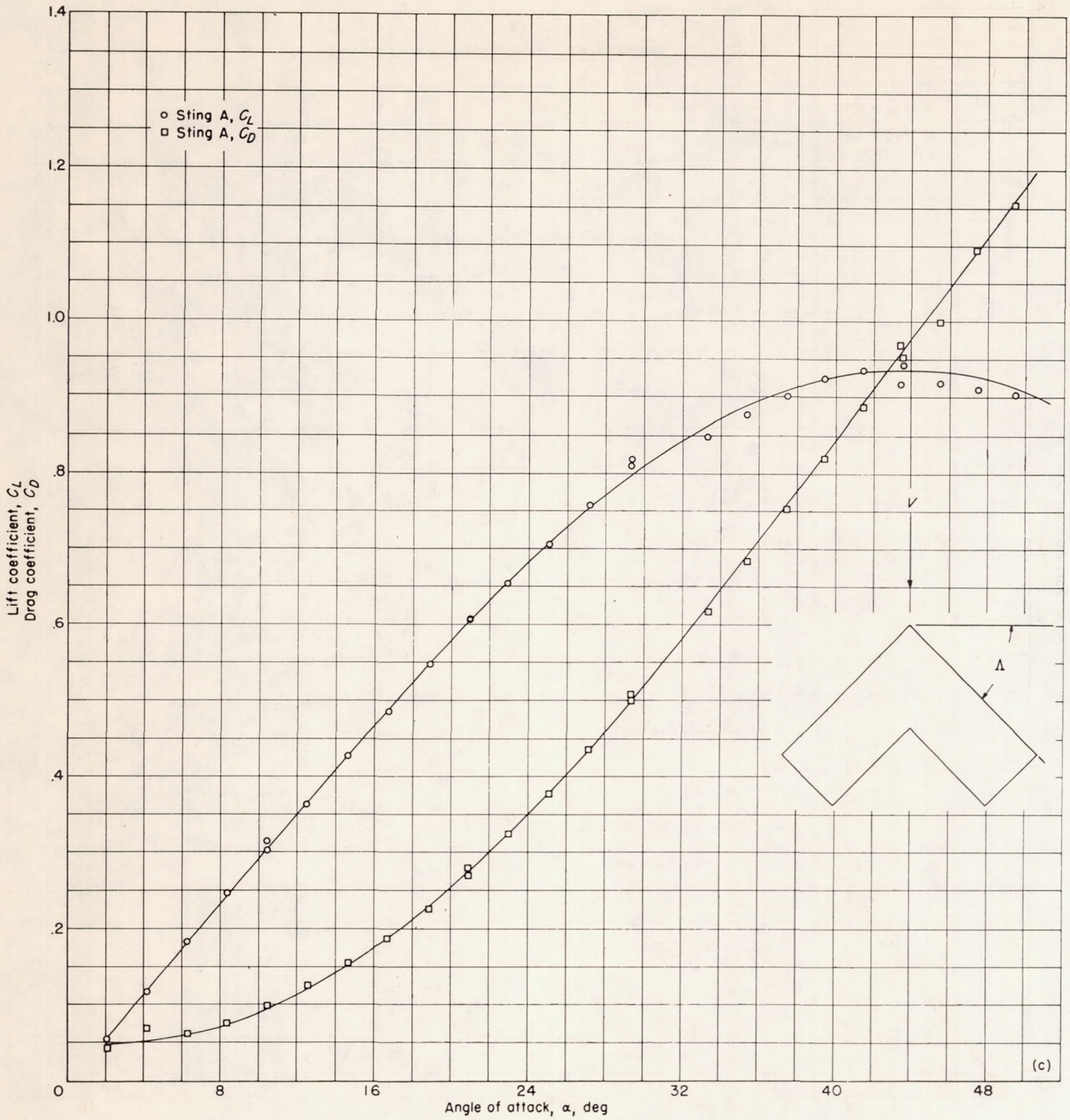

(c) Swept wing; $\Lambda = 45°$.

FIGURE 7.—Continued.

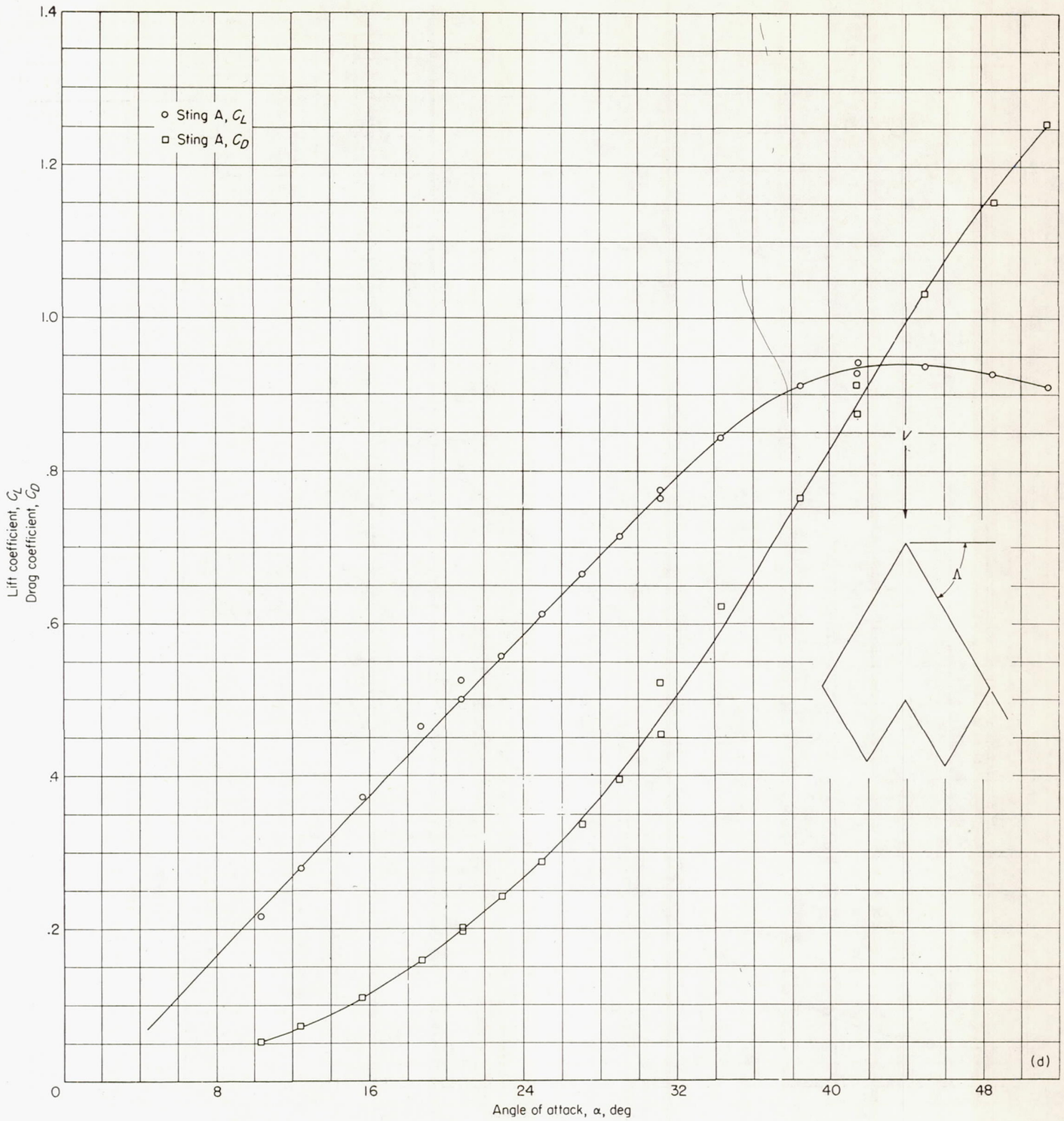

(d) Swept wing; $\Lambda = 63°$.

FIGURE 7.—Continued.

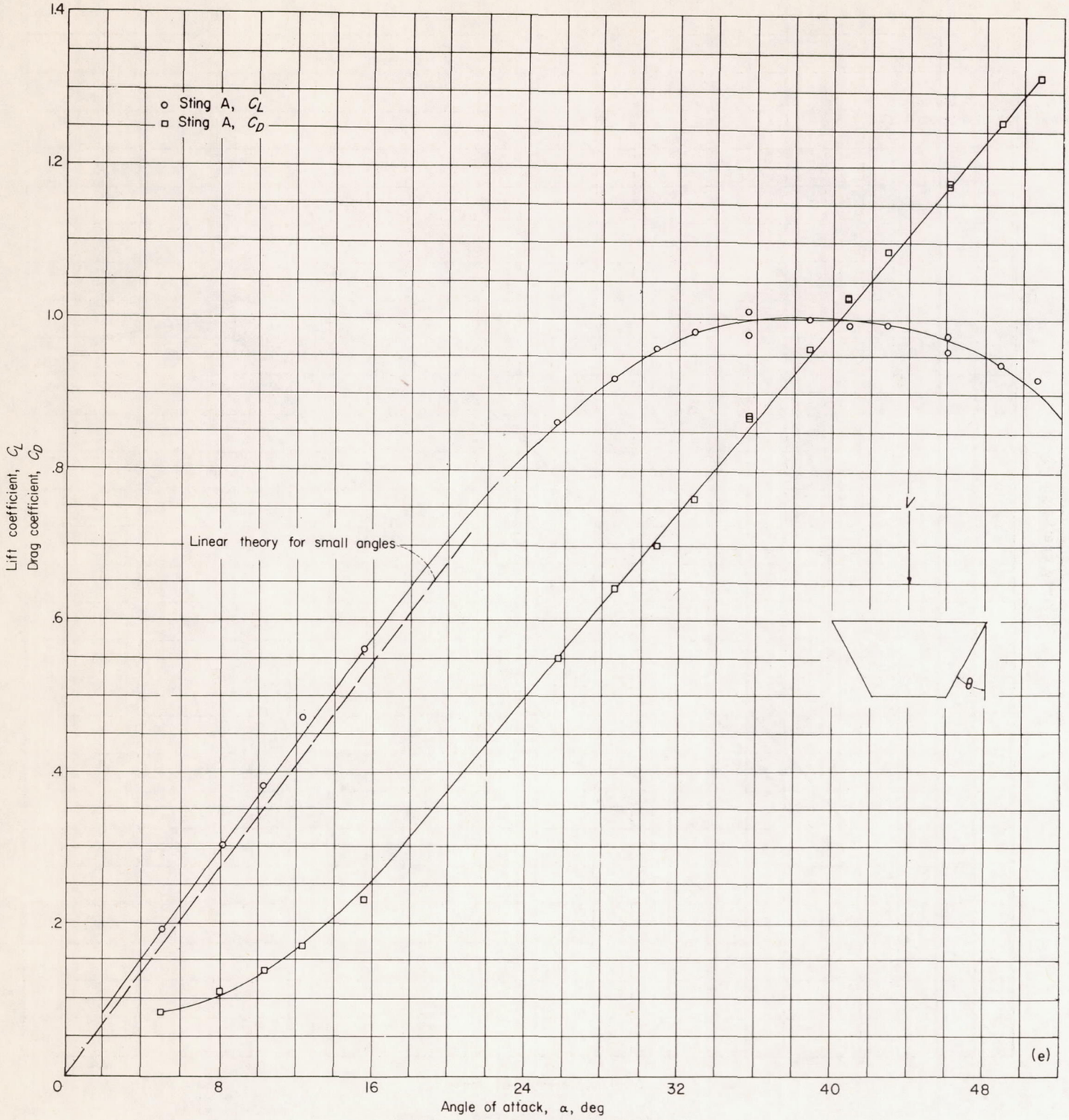

(e) Trapezoidal wing; $\theta = 30°$; tips not beveled.

FIGURE 7.—Continued.

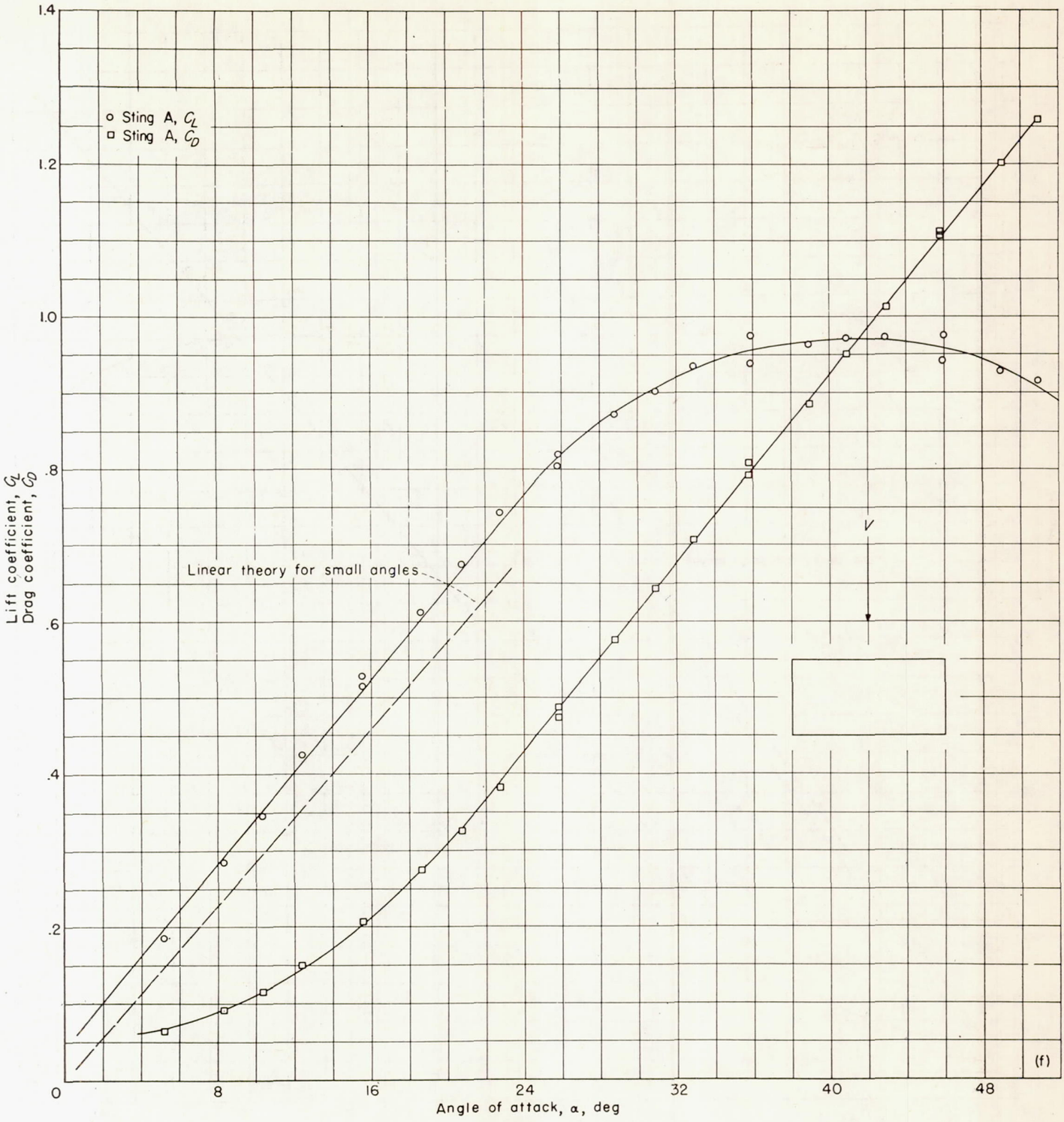

(f) Rectangular wing; $A=1.99$; $t/c=0.09$.

FIGURE 7.—Concluded.

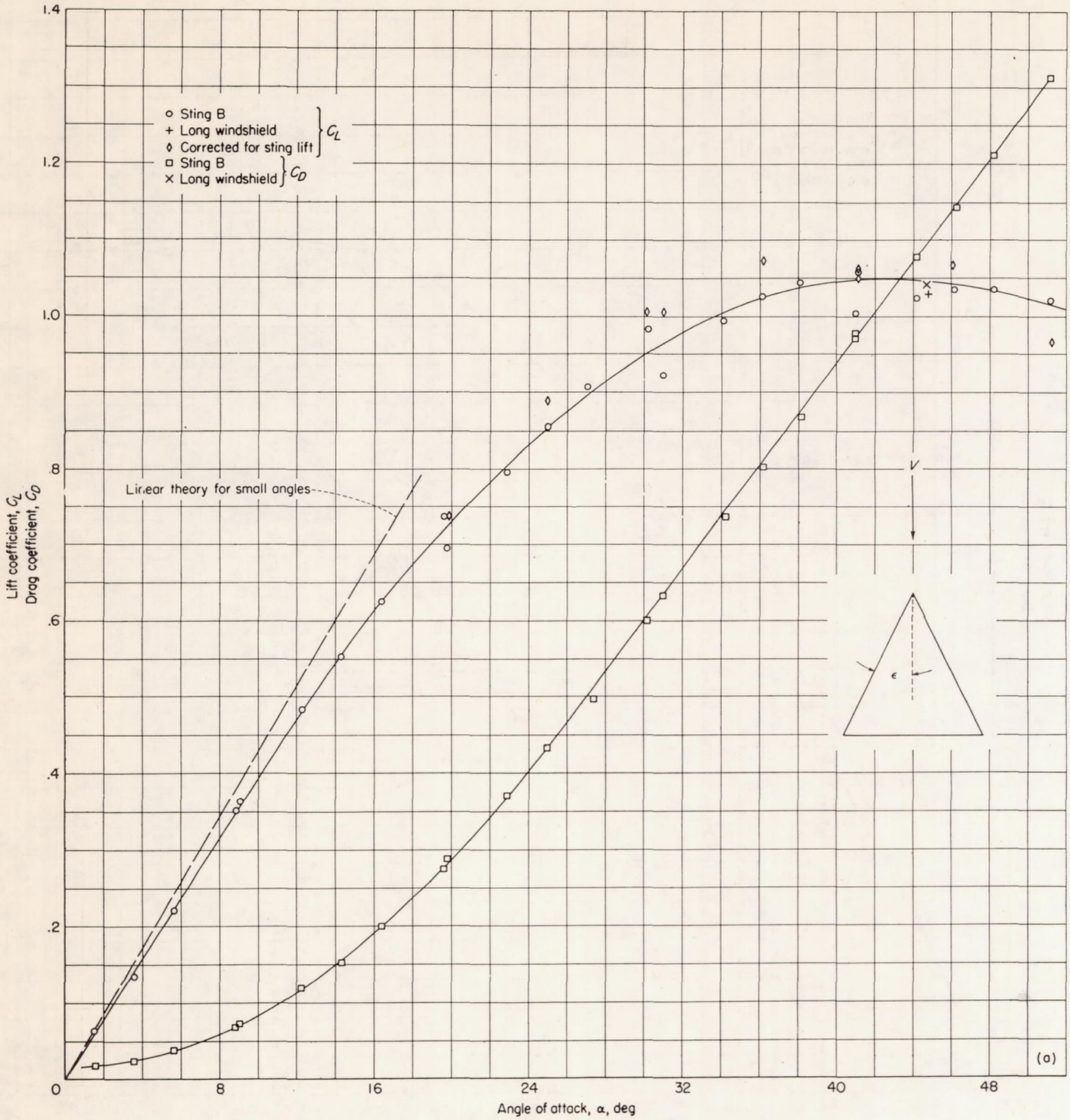

(a) Triangular wing; $\epsilon = 26°$.

FIGURE 8.—Variation of lift coefficient and drag coefficient with angle of attack. $M = 1.55$.

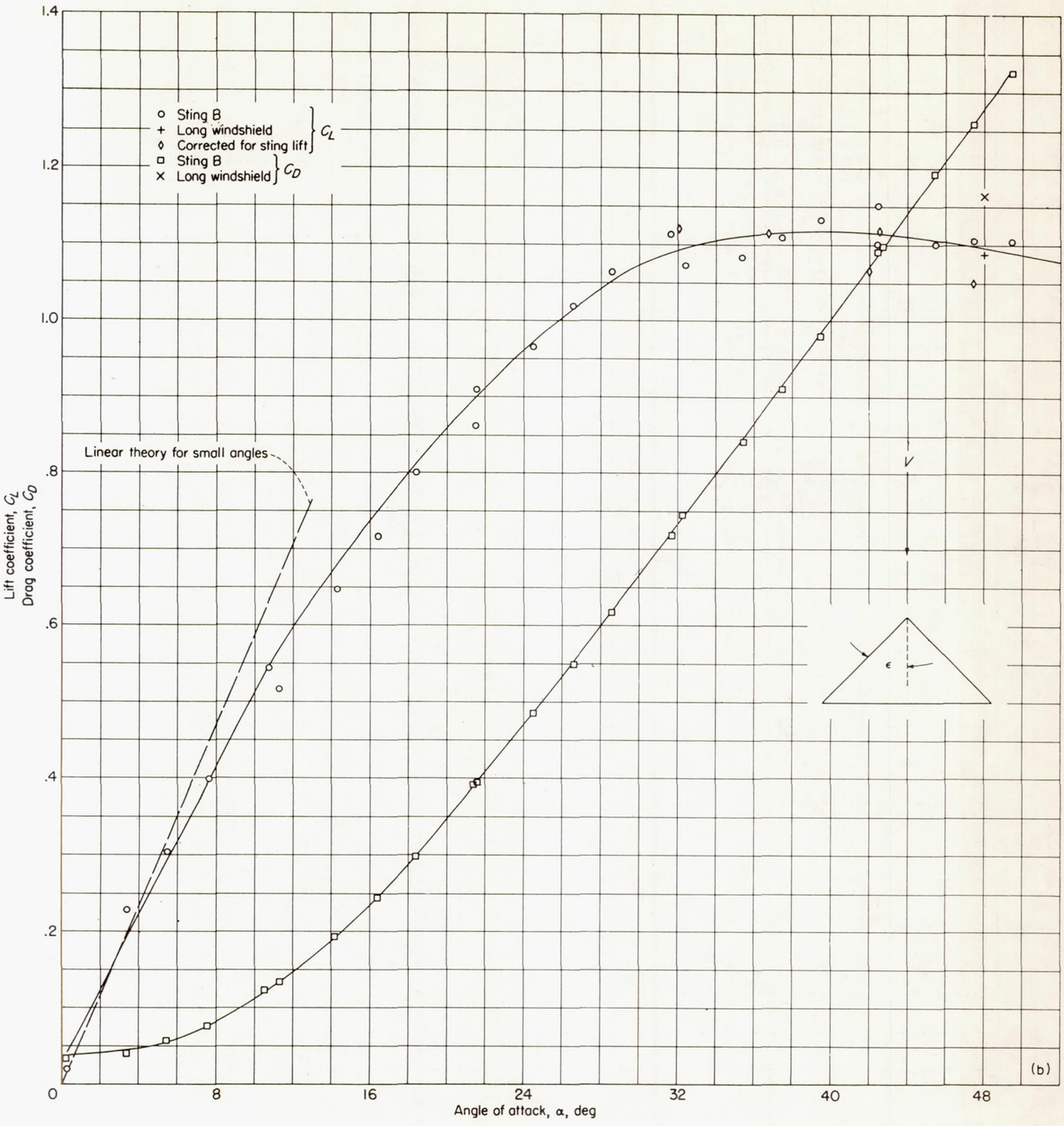

(b) Triangular wing; $\epsilon=45°$.

FIGURE 8.—Continued.

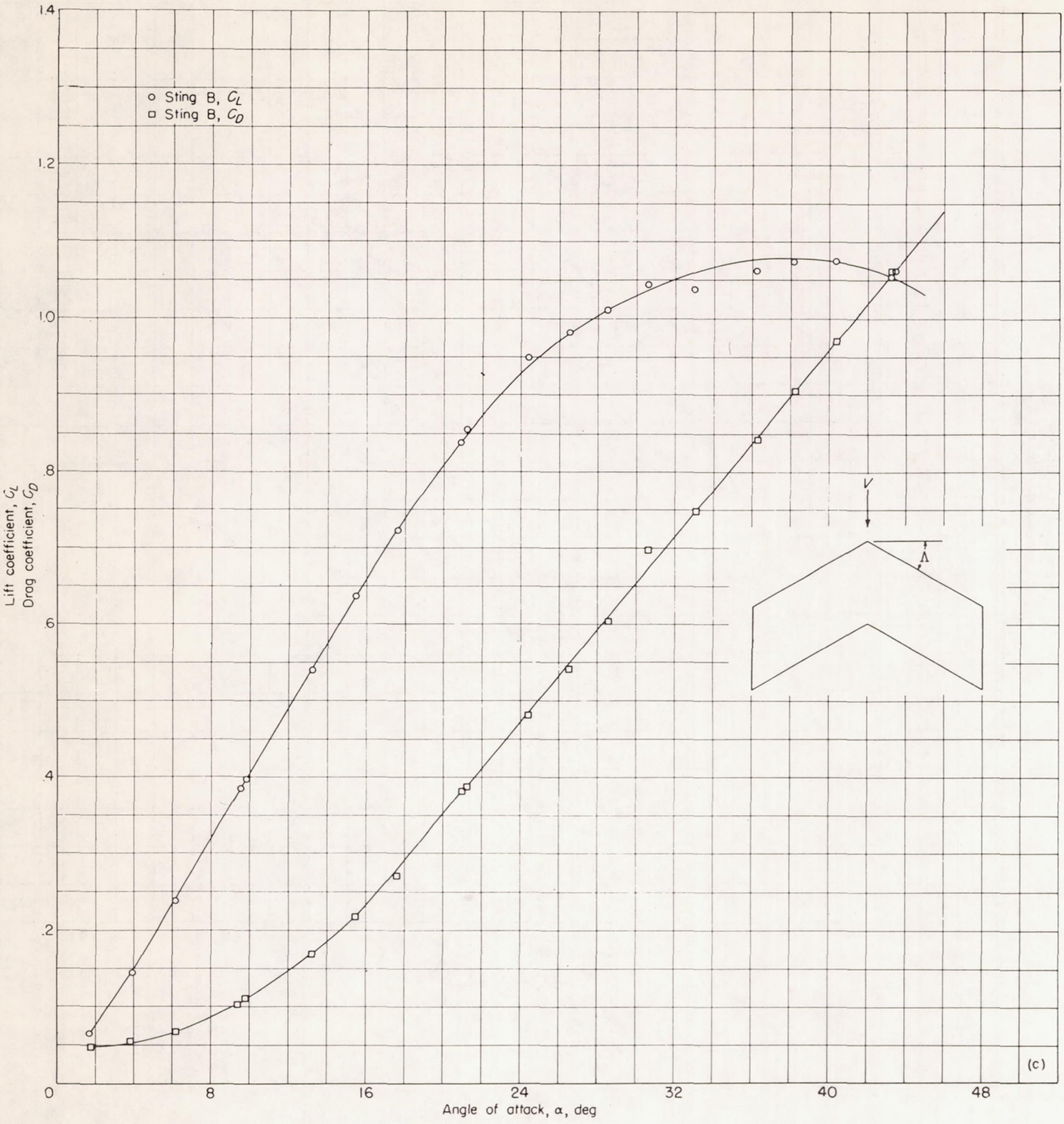

(c) Swept wing; $\Lambda = 36°$.

FIGURE 8.—Continued.

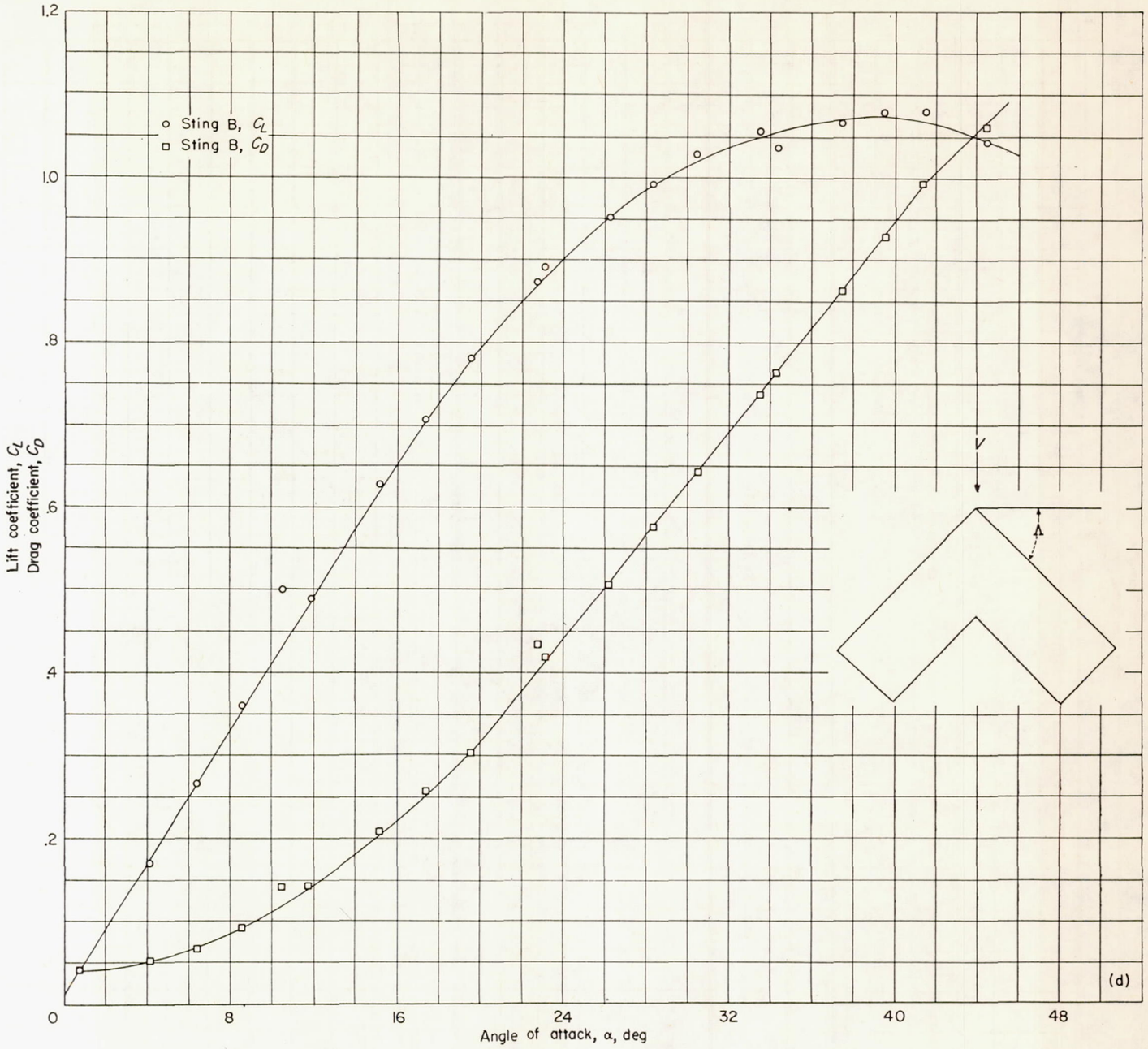

(d) Swept wing; $\Lambda = 45°$.

FIGURE 8.—Continued.

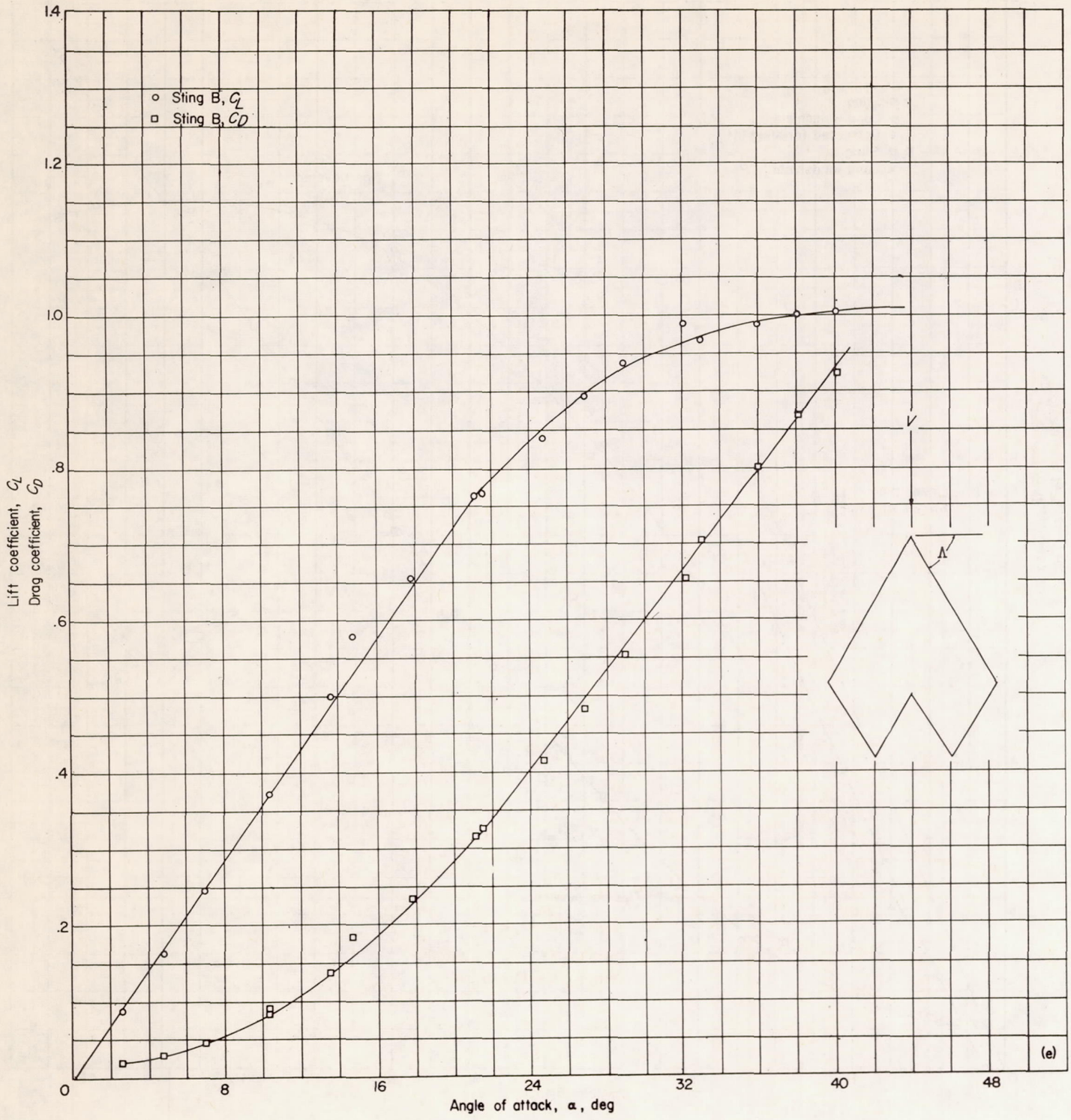

(e) Swept wing; $\Lambda = 63°$.

FIGURE 8.—Continued.

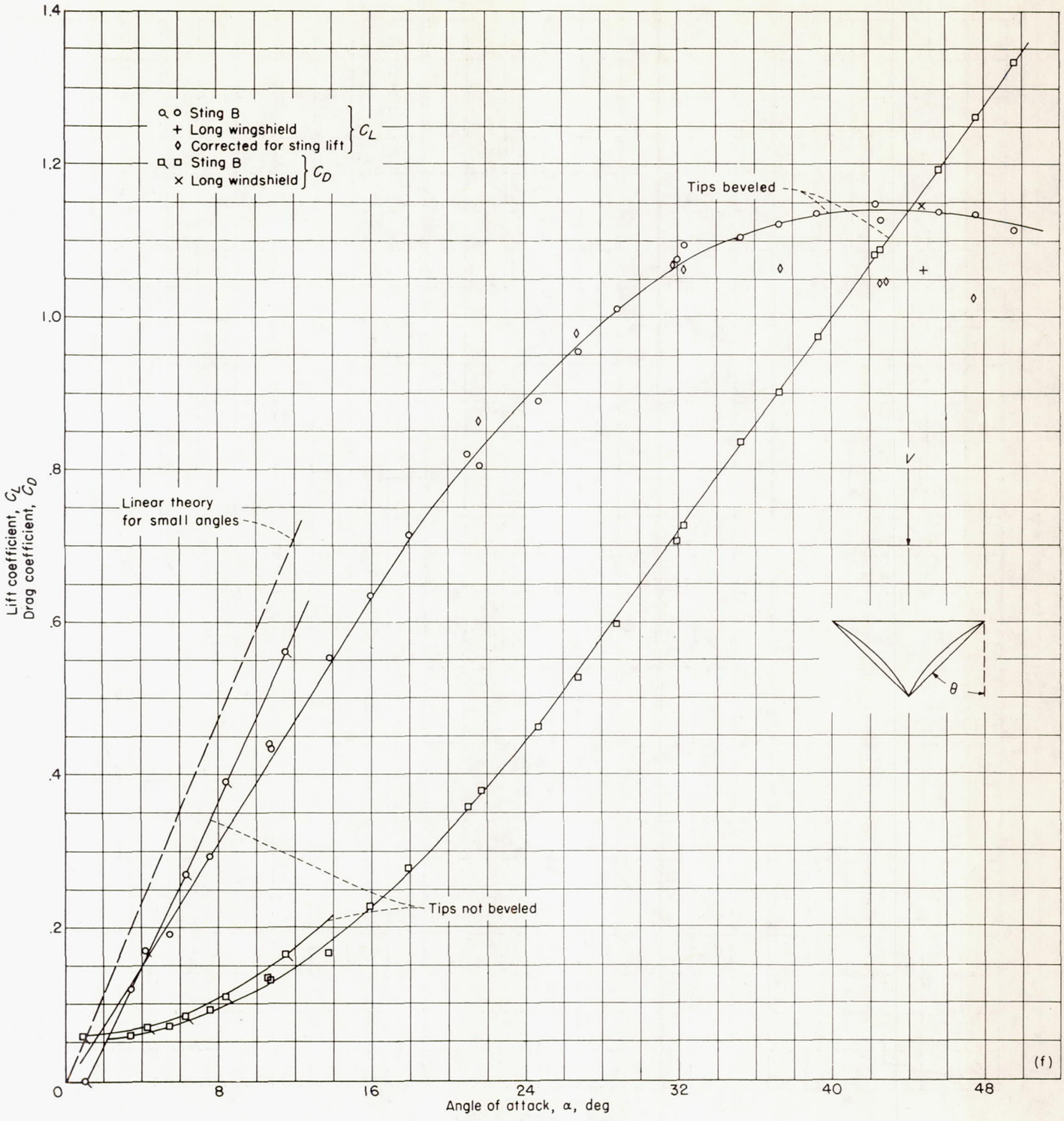

(f) Trapezoidal wing; $\theta = 40°$.

FIGURE 8.—Continued.

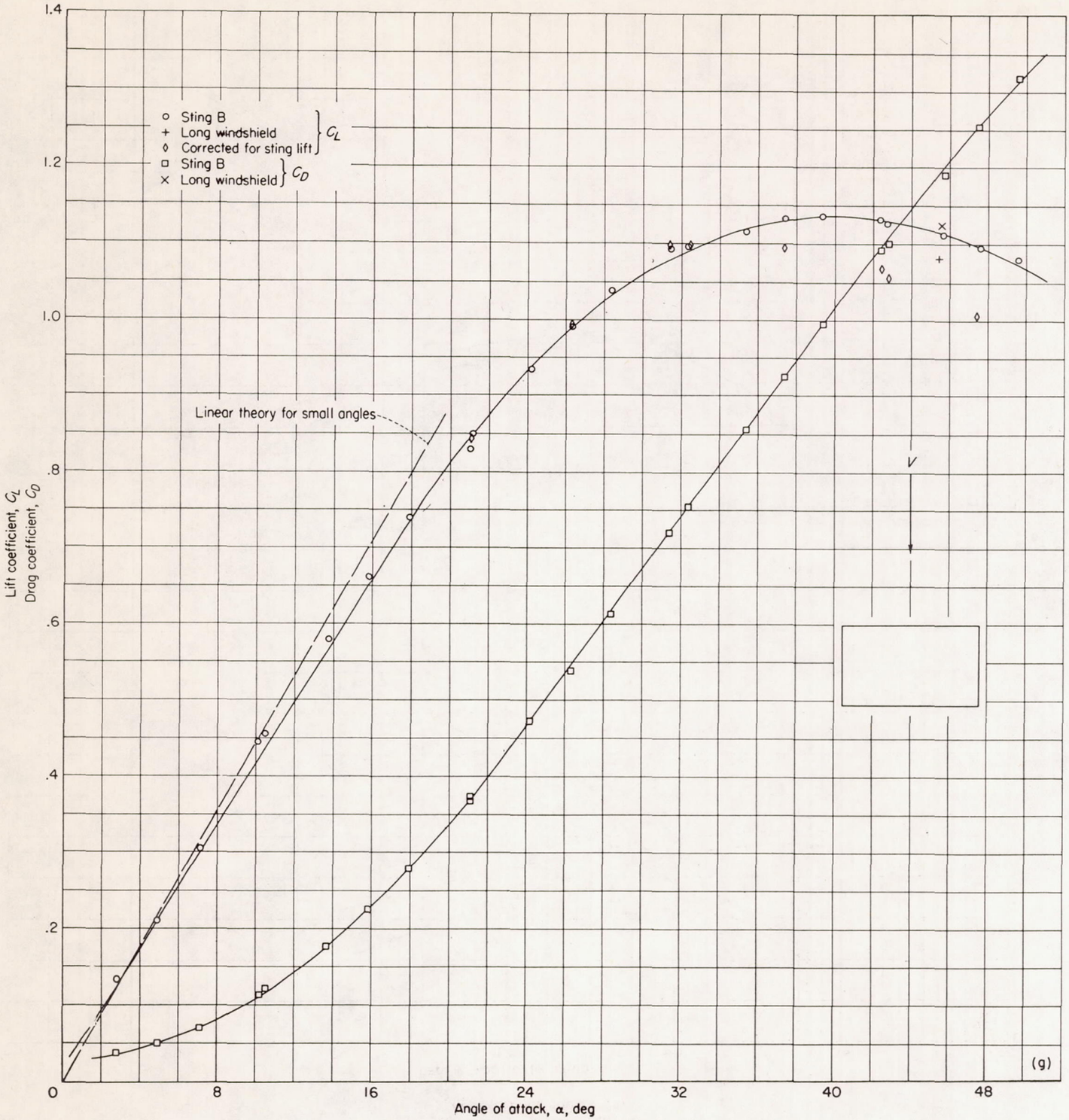

(g) Rectangular wing; $A=1.74$; $t/c=0.06$.

FIGURE 8.—Concluded.

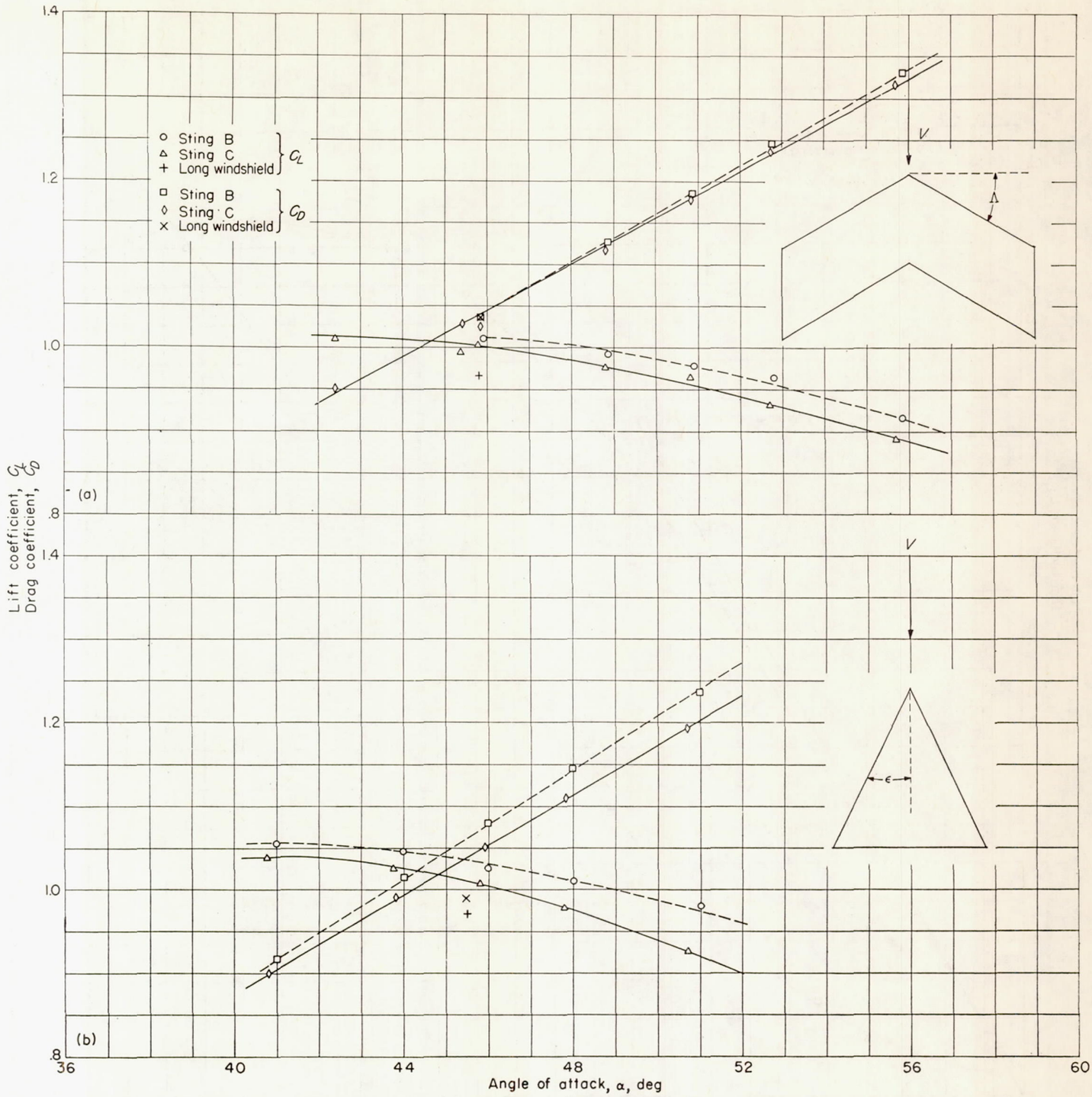

(a) Swept wing; $\Lambda=36°$.
(b) Triangular wing; $\epsilon=26°$.

FIGURE 9.—Variation of lift coefficient and drag coefficient with angle of attack. $M=1.90$.

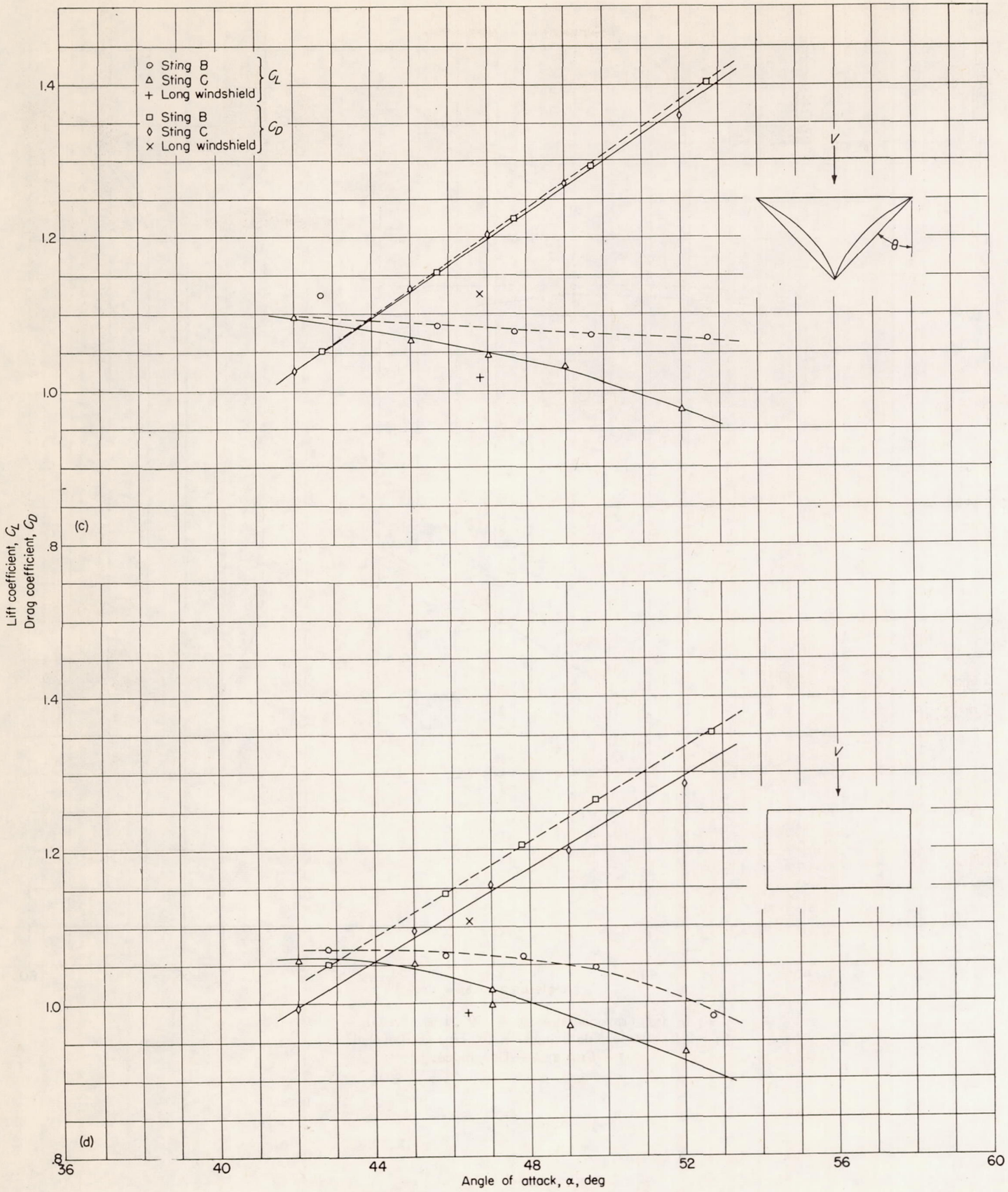

(c) Trapezoidal wing; $\theta=40°$; tips beveled.
(d) Rectangular wing; $A=1.74$; $t/c=0.06$.

FIGURE 9.—Continued.

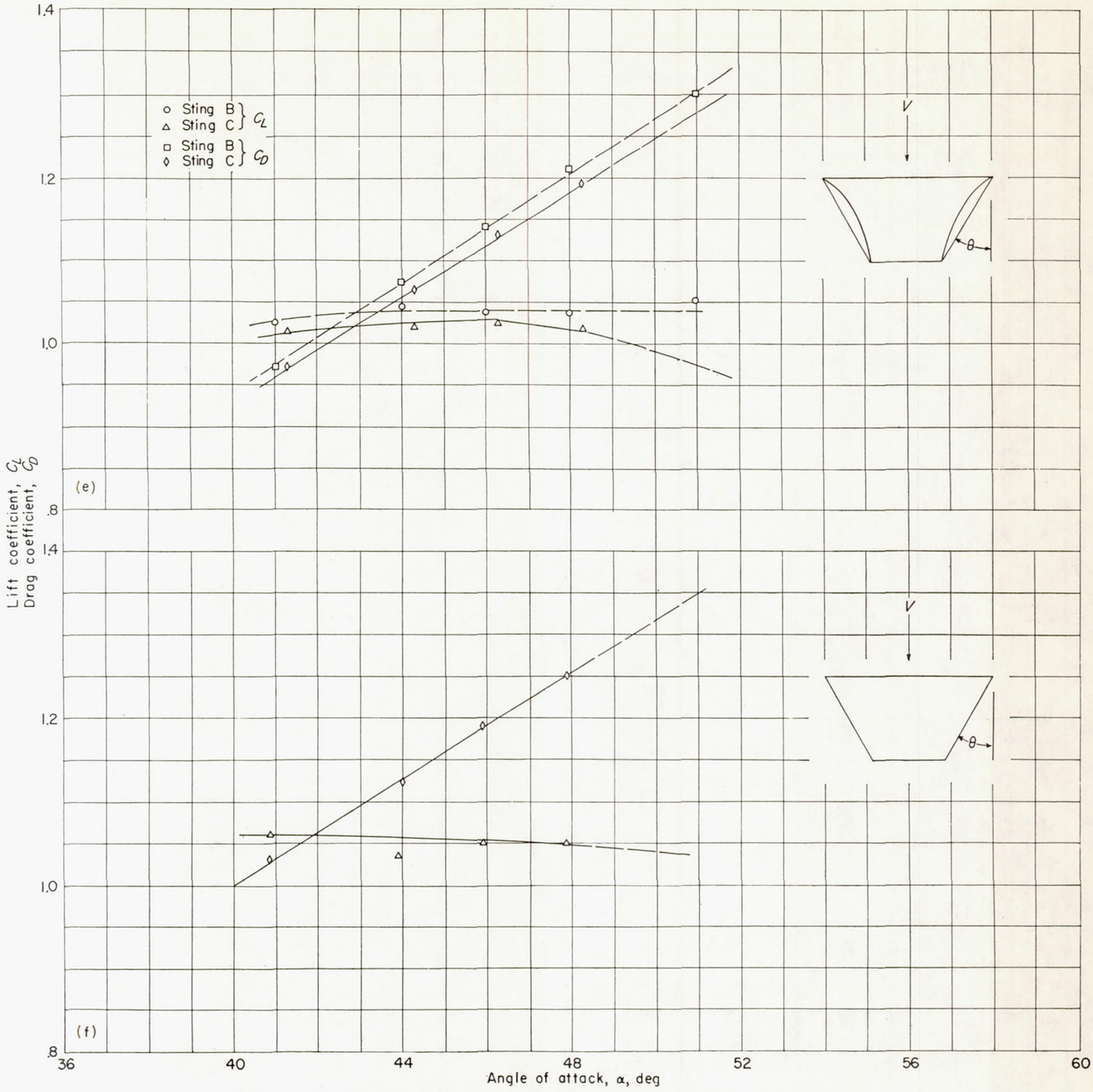

(e) Trapezoidal wing; $\theta=30°$; tips beveled.
(f) Trapezoidal wing; $\theta=30°$; tips not beveled.
FIGURE 9.—Concluded.

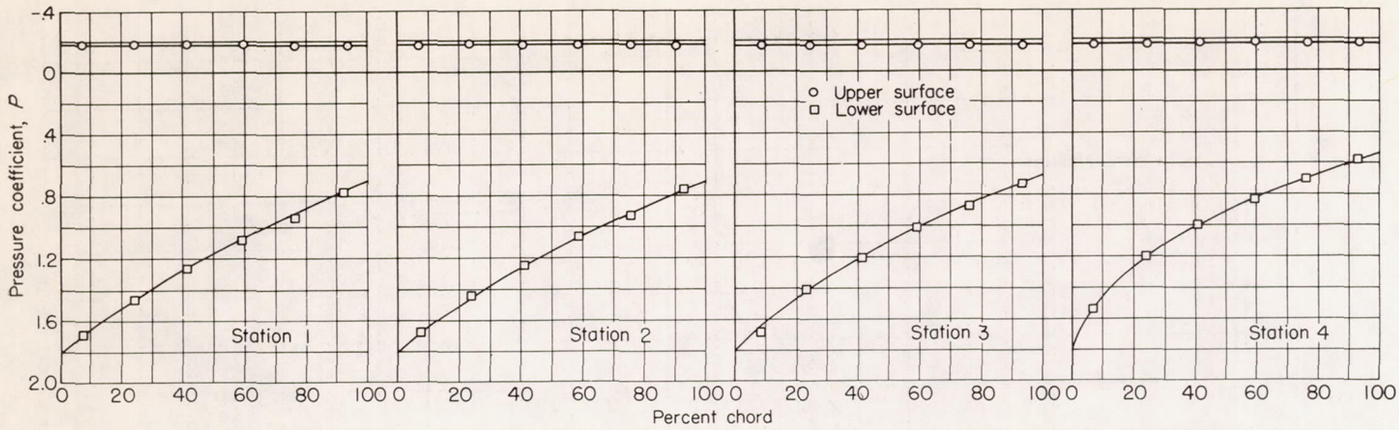

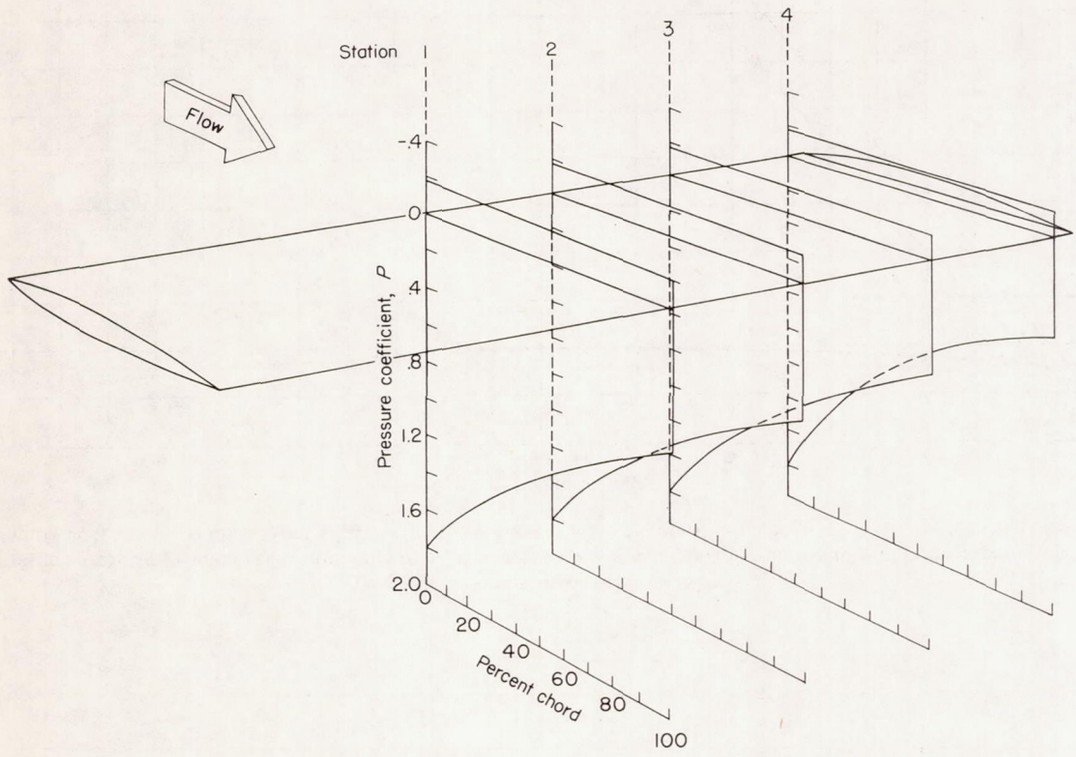

FIGURE 10.—Typical pressure diagrams in the region of maximum lift.
Rectangular wing; $A=2.29$; $t/c=0.09$; $\alpha=42°$; $M=2.40$.

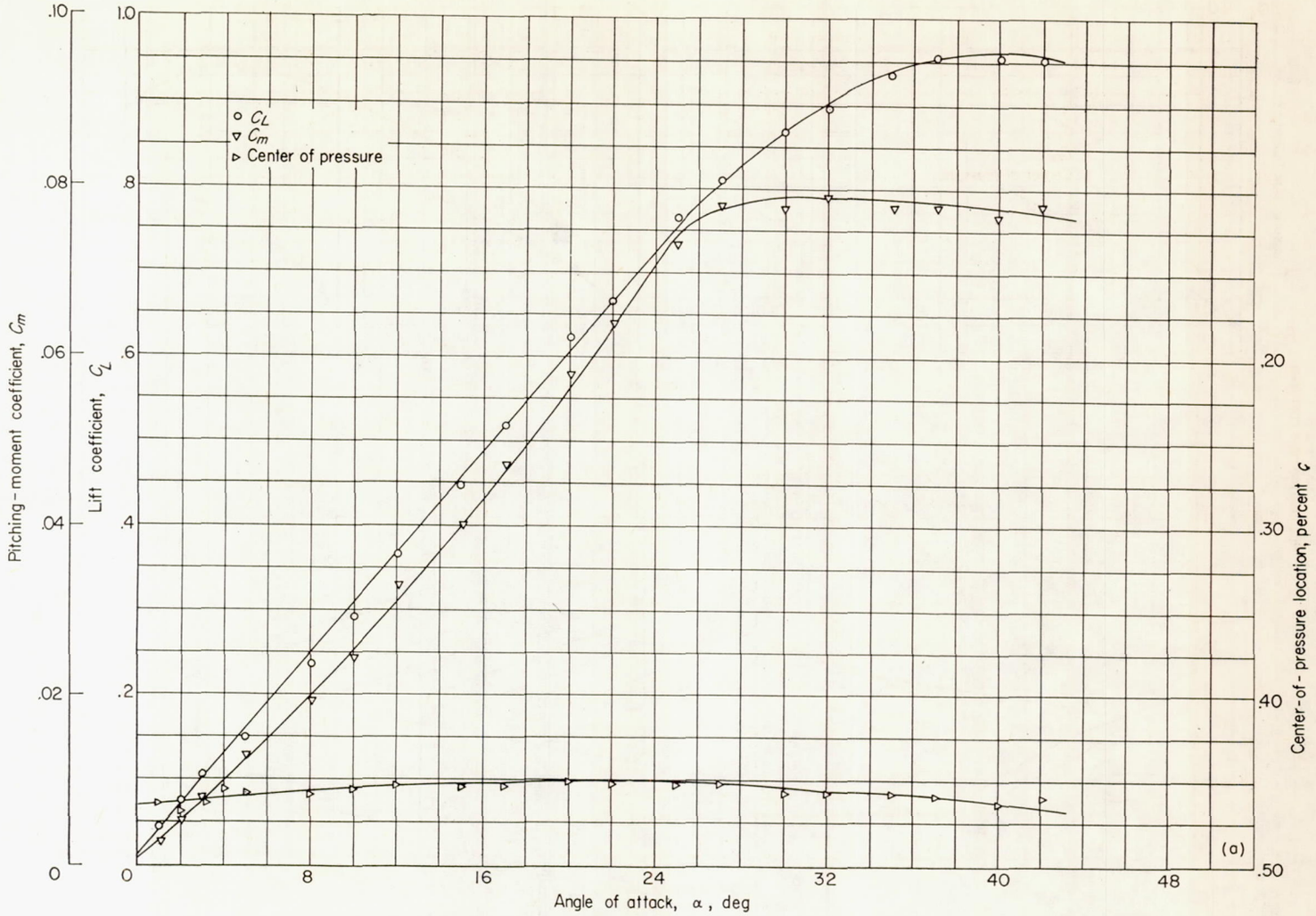

(a) Rectangular wing; $A=2.29$; $t/c=0.09$; Reynolds number, 0.45×10^6; C_m determined about $0.5c$ point.

FIGURE 11.—The variation of lift and pitching-moment coefficients and center-of-pressure locations with angle of attack as obtained from integration of pressure measurements. $M=2.40$.

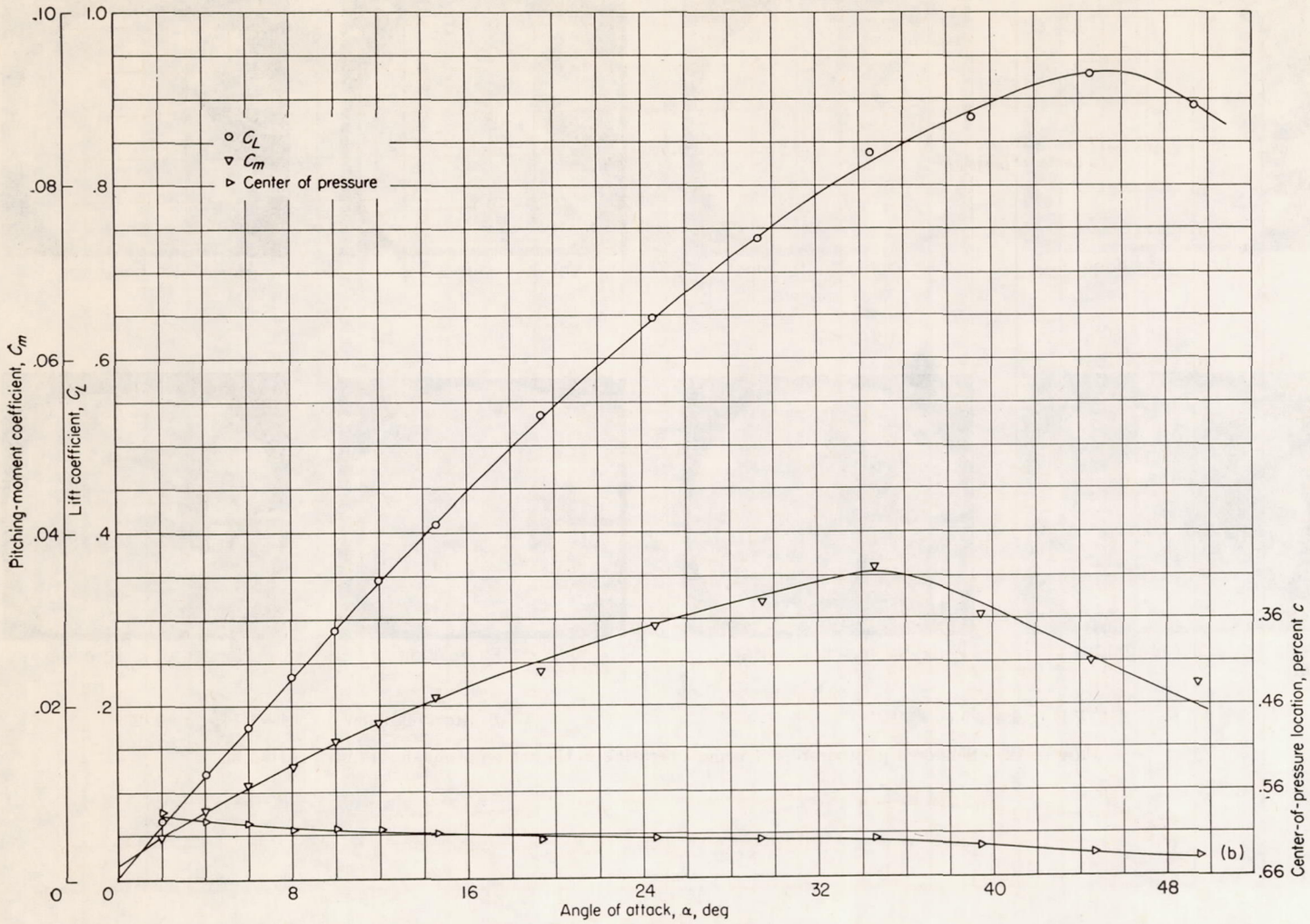

(b) Triangular wing; $\epsilon=31.5°$; $t/c=0.10$; Reynolds number, 0.78×10^6; C_m determined about $0.66c$ point.

FIGURE 11.—Concluded.

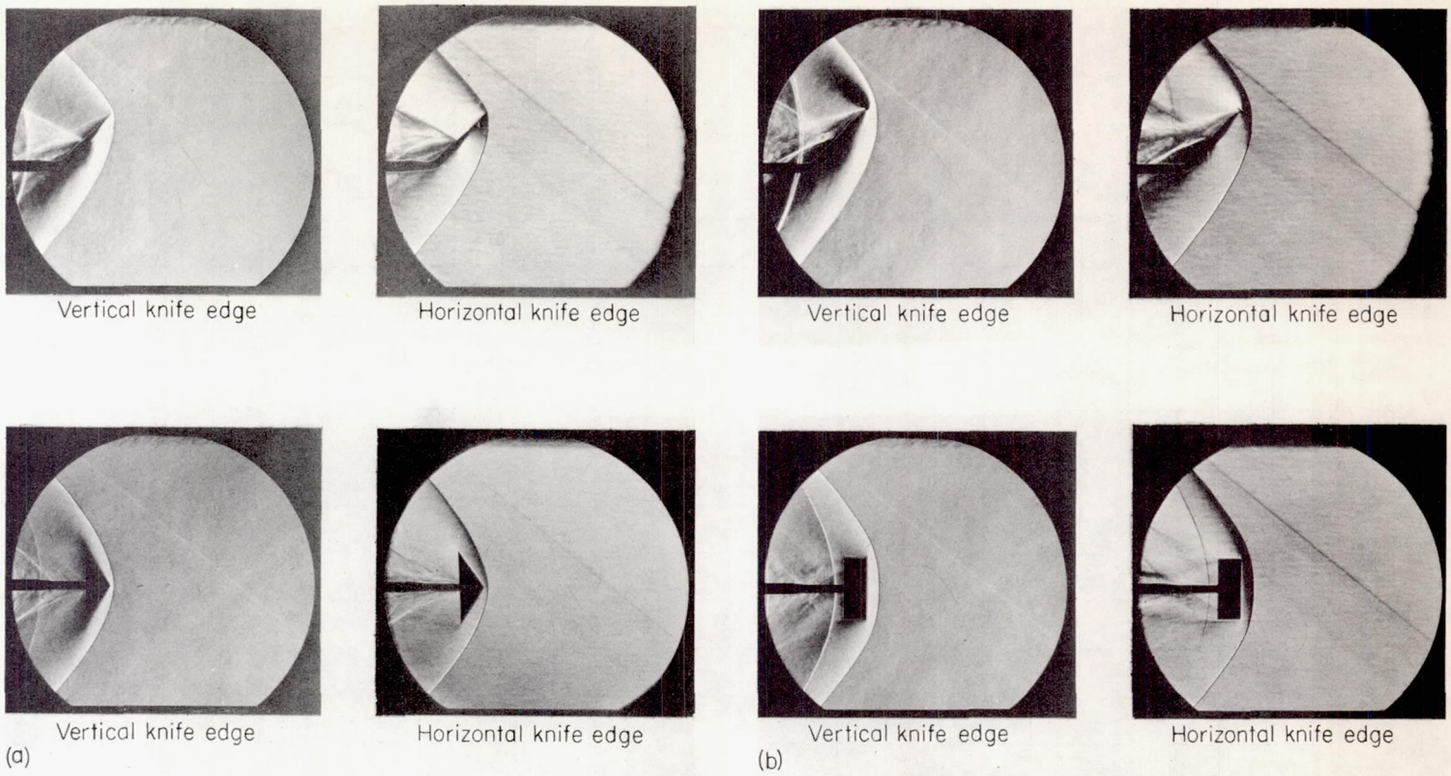

(a) Triangular wing; $\epsilon=45°$.

(b) Rectangular wing; $A=1.74$; $t/c=0.06$.

FIGURE 12.—Schlieren photographs of wings operating in the region of maximum lift. $M=1.55$.

☆ U.S. GOVERNMENT PRINTING OFFICE : 1959 O—506454